Late Quaternary paleohydrology of the central Atacama Desert (lat 22°–24°S), Chile

Jason A. Rech*
Jay Quade
Department of Geosciences and Desert Laboratory, University of Arizona, 1675 West Anklam Road, Tucson, Arizona 85745, USA

Julio L. Betancourt
U.S. Geological Survey and *Desert Laboratory, University of Arizona, 1675 West Anklam Road, Tucson, Arizona 85745, USA*

ABSTRACT

In northern Chile, precipitation in the High Andes (>3500 m) recharges groundwater systems that flow down the Pacific slope and feed large aquifers in the hyperarid Atacama Desert. Wetlands, which are often found along the base of the Andes, mark locations where the water table intersects the land surface. At these locations, paleo–wetland deposits, which are present as terraces between 3 and 20 m above modern wetlands, record past water-table heights along the Andean front and are used to reconstruct changes in groundwater discharge. Paleo–wetland deposits in the central Atacama Desert (lat 22°–24°S) record an episode (>15.4–9 ka) of high water tables followed by an episode (8–3 ka) of moderately high water tables. Elevated water tables result from increased groundwater discharge and ultimately from enhanced recharge in the Andes. The concordance of results from three separate hydrologic systems suggests that changes in groundwater discharge and recharge are regional and reflect climatic fluctuations. This interpretation is supported by close agreement with other paleoclimatic records in the region. The periods of greater groundwater discharge were separated by episodes (9–8 and 3–0 ka) of significant groundwater lowering and stream incision, implying greatly diminished discharge.

The central Atacama and Andes (lat 22°–24°S) receive precipitation mainly from moist air masses transported from the Amazon Basin by the South American Summer Monsoon (SASM). Increases in groundwater recharge are therefore thought to reflect an increase in the frequency and/or moisture content of SASM air masses crossing the Andes. Fluctuations in SASM precipitation have previously been linked to summer insolation in the Southern Hemisphere. The wettest period in the central Atacama (>15.4–9 ka), however, coincides with a minimum in austral-summer insolation at 10 ka, suggesting that regional summer insolation is not a dominant influence on the SASM. Instead, intensification of the SASM may be linked to extraregional forcings such as the Walker Circulation.

Keywords: Atacama Desert, wetlands, springs, paleohydrology, South America.

INTRODUCTION

The tropics are thought to play a fundamental role in climate change because of their ability to force rapid changes over broad regions of the Earth (Cane and Clement, 1999; Clement and Cane, 1999; Kerr, 2001). Notwithstanding this importance, tropical paleoclimatic studies are sparse compared to those at higher latitudes. This disparity has encouraged a reliance on global methane concentrations (Severinghaus and Brook, 1999) and coupled ocean-atmosphere circulation models (Bush and Philander, 1998; Hostetler and Mix, 1999; Pinot et al., 1999) for making inferences about past tropical oceanic and atmospheric circulation. Well-dated records of tropical precipitation are becoming increasingly necessary to set model limits, to isolate source regions for global methane, and ultimately to determine the relationship of past circulation changes both among separate regions in the tropics and between the tropics and high latitudes. The South American Summer Monsoon (SASM) represents an important component of the tropical circulation system and provides one avenue for testing these relationships.

Today the SASM influences a large region of South America, including the Amazon Basin, central Andes, and Altiplano. Continental heating in summer drives deep convection over the Amazon Basin, bringing moisture into this region from the equatorial Atlantic via the trade winds (Fig. 1). The trades are deflected southeast once they reach the Andes, creating a low-level northwesterly jet that transports tropical moisture from the Amazon toward the Gran Chaco region (lat 20°–25°S) (Nogués-Peagle and Mo, 1997; Zhou and Lau, 1998). A thermal low develops over the Gran Chaco region as maximum solar heating migrates south at the end of the austral summer. When the Gran Chaco low is fully developed, the SASM is at its strongest seasonal intensity (Zhou and Lau, 1998).

Periodically increasing Southern Hemisphere seasonal insolation has been presumed to be the dominant control on the intensification of the SASM over orbital time scales (Martin et al., 1997; Seltzer et al., 2000; Cross et al., 2000; Baker et al., 2001a, 2001b; Bobst et al., 2001). High lake levels and glacial advances during the Last Glacial Maximum (LGM) in the central Andes led researchers to suggest that the summer-insolation maximum at ~21 ka intensified the SASM (Seltzer et al., 2000; Baker et al., 2001b). Conversely, on the Bolivian Altiplano (lat 15°–22°S), lake desiccation and glacial retreat by ca. 14 ka have been attributed to the summer-insolation minimum at ~10 ka (Servant et al., 1995; Clayton

*E-mail: jrech@geo.arizona.edu.

GSA Bulletin; March 2002; v. 114; no. 3; p. 334–348; 15 figures; 1 table.

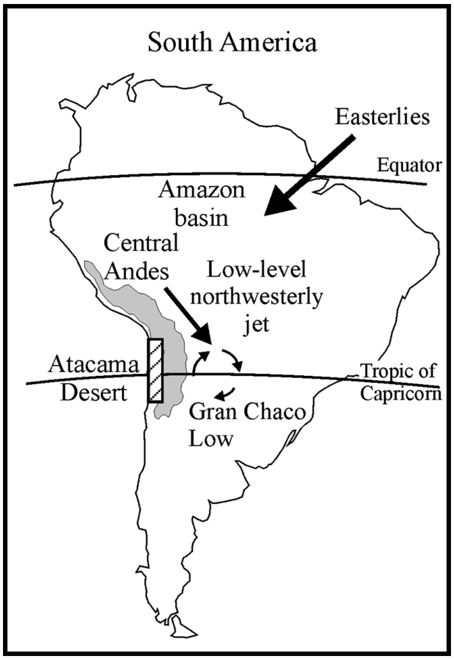

Figure 1. Summer atmospheric circulation patterns responsible for the transport of moisture to the Atacama Desert.

and Clapperton, 1997; Sylvestre et al., 1999; Baker et al., 2001a, 2001b). These inferred wet and dry periods are out of phase with many paleoclimatic records from the Amazon, which identify a dry LGM and wet late glacial and Holocene (Ledru, 1993; Colinvaux et al., 1996; Harris and Mix, 1998). This discrepancy led Martin et al. (1997) to argue that decreased summer-insolation values limited the southward expansion of the SASM, causing the southernmost tropics and northern subtropics to desiccate while parts of the Amazon Basin became wetter owing to a prolonged summer wet season.

Paleoclimatic records from the Pacific slope of the central Andes and Atacama (lat 22°–24°) can be used to test these hypotheses linking seasonal insolation effects to SASM intensity. In this region, paleoclimatic records should reflect drying between 13 and 10 ka if this model of summer-insolation forcing over the South American tropics is correct. Most regional records, however, identify a wet period from ca. 16 to 9 ka, coincident with the orbitally determined minimum in austral-summer insolation (Grosjean, 1994; Grosjean et al., 1995; Geyh et al., 1999; Betancourt et al., 2000). This wet phase, which is generally concordant with records from the Amazon, was also demonstrated to result from summer precipitation (Betancourt et al., 2000). There is no obvious reason why the Amazon and Atacama should have been wettest during the late Glacial to early Holocene (16–9 ka), while the intervening Bolivian Altiplano experienced maximum wetness during the LGM (25–16 ka).

In this paper we present evidence from well-dated fossil spring and fluvial wetland deposits that document the timing of wet and dry phases in the central Atacama Desert. This evidence calls into question whether paleoclimatic boundaries existed between the Amazon and Altiplano, and between the Altiplano and the central Atacama, and suggests that regional summer insolation is not the dominant control on SASM intensification. These results have important implications regarding (1) the forcing mechanisms for climate change in the tropics and (2) the climatic teleconnections between the Northern and Southern Hemispheres.

STUDY AREA

The Atacama Desert, perhaps the driest place on Earth, is located between the central Andes and Pacific Ocean in southern Peru and northern Chile (Fig. 1). The core of the Atacama receives virtually no precipitation (<5 mm/yr), does not support vascular plants, and probably has been unaffected by Quaternary climate change. During the Quaternary, however, vegetation has expanded and contracted across the eastern, upper margin of the Atacama (~2600 m) in step with fluctuations in saline and freshwater lake levels and groundwater discharge (Betancourt et al., 2000). Evidence for changes in groundwater discharge is preserved in conspicuous paleo–wetland deposits that mark past water-table heights along groundwater flow paths from the Andes to aquifers in the Atacama.

We studied paleo–wetland deposits at several locations in the central Atacama Desert (lat 22°–24°S) of Chile (Fig. 2). Tilomonte Springs (lat 23°47′S, long 68°05′W, ~2500 m), a complex of springs and related streams and wetlands, is located in the southeast part of the Salar de Atacama basin near the base of the Andes. The Río Loa (lat 22°20′ S, long 68°40′W, ~2500 m) and Río Salado (lat 22°20′S, long 68°34′W, ~2500 m), perennial low-energy streams that drain the Andes, are located in the Calama basin ~150 km north-northwest of Tilomonte Springs. The combined results from these study areas, plus a reinterpretation of paleo–wetland deposits previously reported at Quebrada (= canyon) Puripica (Grosjean et al., 1997), provide a regional record of paleohydrologic changes.

PRECIPITATION IN THE CENTRAL ATACAMA AND SOUTHERN ALTIPLANO

The central Atacama and southern Altiplano are situated at the distal end of the tropical precipitation belt and receive most of their precipitation during summer from air masses that originate in the Atlantic (Miller, 1976; Zhou and Lau, 1998). Precipitation in this region ranges from ~25 mm/yr at the base of the Andes (~2500 m) to ~150 mm/yr above 4000 m (Fig. 3A) (Dirección General de Agua, no date). Stations below ~3000 m receive up to 40% of their annual precipitation during the austral winter (May through August) from Pacific source regions (Fig. 3B) (Vuille and Ammann, 1997; Vuille and Baumgartner, 1998; Vuille, 1999), whereas stations above ~3000 m receive >85% of their annual precipitation during the austral summer (December through March = DJFM) (Fig. 3, C–E). This seasonal precipitation pattern for stations above 3000 m matches that of stations on the Bolivian Altiplano to the north, e.g., Sajama at lat 18°S (Fig. 3F), and suggests that the same large-scale changes in atmospheric circulation responsible for precipitation over Sajama (Hardy et al., 1998; Vuille et al., 1998; Vuille, 1999) are also dominant in the central Atacama (lat 22°–24°S). Winter moisture imbedded in Pacific air masses dominates annual precipitation totals south of ~25°S.

Summer precipitation on the southern Altiplano and the central Atacama is directly linked to solar heating on the Altiplano and the location and strength of the Bolivian High (Aceituno and Montecinos, 1993; Vuille et al., 1998; Lenters and Cook, 1999; Vuille, 1999). The Bolivian High is an anticyclonic vortex in the upper troposphere that results from deep convection and latent-heat release over the Amazon Basin (Silva Dias et al., 1983; Lenters and Cook, 1997). An intensification and southward displacement of the Bolivian High disturbs middle and upper tropospheric westerly wind flow and allows for enhanced easterly flow and increased moisture influx from the interior of the continent. Both weakening and northward displacement of the Bolivian High are usually associated with dry periods on the Altiplano. Altiplano climate, especially in the western region, has also been linked to the Southern Oscillation (SO) and SSTs (sea-surface temperatures), with cooler atmospheric temperatures, a southward displacement of the Bolivian High, easterly wind anomalies, and above-average precipitation occurring during La Niña events (Aceituno, 1988; Ronchail, 1995; Vuille, 1999; Vuille et al., 2000).

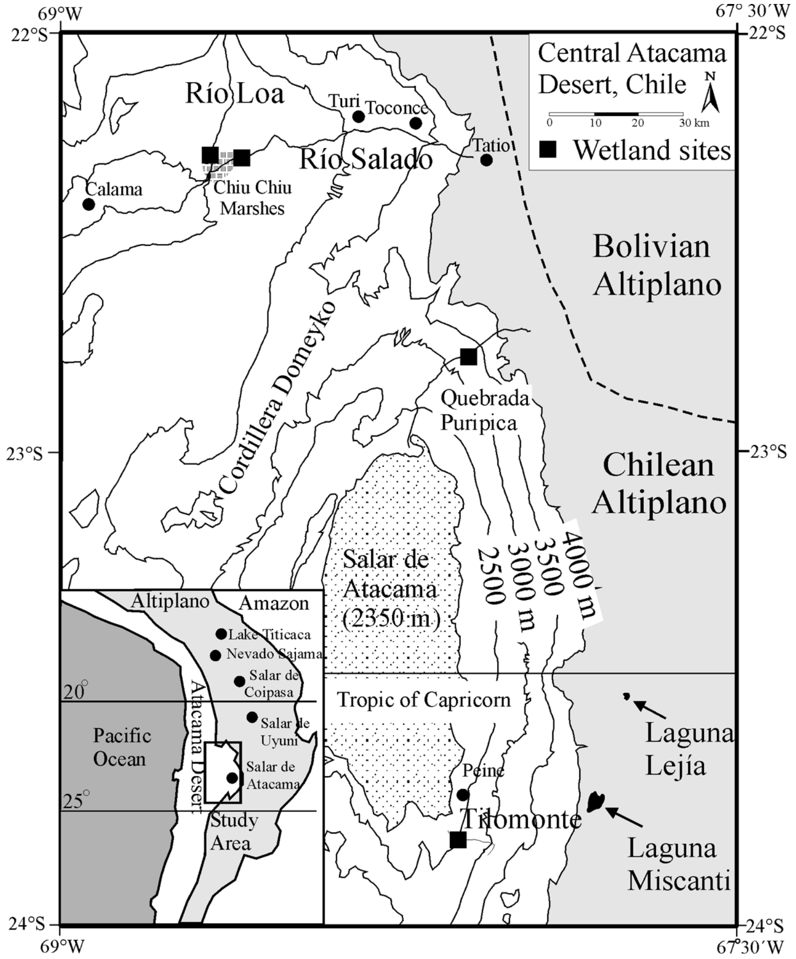

Figure 2. Location of spring and wetland sites in the central Atacama Desert, Chile. Inset shows Andean Altiplano (15°–30°S) and locations of key paleoclimatic records.

In contrast, El Niño events are associated with warmer atmospheric temperatures, a northward displacement of the Bolivian High, westerly wind anomalies, and below-average precipitation.

ANALYSIS OF PALEO–WETLAND DEPOSITS

Wetlands form where the modern water table intersects the land surface. Our study areas on the Río Loa and Río Salado are part of the Chiu Chiu marshes, located at the juncture of the Andes and the Calama Basin (Fig. 2). Both the Río Loa and Río Salado are perennial streams fed by groundwater (Aravena and Suzuki, 1990). Tilomonte Springs and Quebrada Puripica are located on the steep Pacific slope of the Andes and represent surficial expressions of groundwater flow paths that go from recharge areas at high elevations to aquifers in the Atacama Desert. Hence, water tables are higher at these locations than in areas immediately adjacent.

Streams in these hydrologic systems are small (1–3 m wide), shallow (<1 m deep), low-energy, and contain an abundance of hydrophytic vegetation such as pampa grasses (*Cortaderia*) and sedges (Fig. 4). Phreatophytes are dominant in areas away from the main stream channel where the water table is below the surface. Sediment assemblages associated with wetlands include diatomite, organic mats, tufa ($CaCO_3$), and sinter (SiO_2) along the main stream channel, diatomite and organic mats in local depressions, and silts and sands in overbank deposits (Fig. 4). Some sand and gravel bars are present in the main channel.

Paleo–wetland deposits, which are found on the margin of modern wetlands, generally consist of fining-upward sequences containing alluvial sand and gravel, silt, biogenic deposits such as organic mats and diatomite, and chemical precipitates such as tufa and siliceous sinter. The presence of thick (>50 cm) biogenic deposits and chemical precipitates in paleo–wetland deposits clearly mark past water-table heights. Also, these thick, often finely bedded (2–5 cm), deposits indicate that water-table rise preceded sedimentation.

We argue that increases in water-table height should be a significant means of accommodating increased recharge, particulartly where aquifers are unconfined. As indicated by Darcy's law, an increase in the cross-sectional area of the flow path results in greater groundwater discharge if the hydraulic gradient and hydraulic conductivity are held constant. The hydraulic conductivity also has remained relatively constant, as shown by the fact that paleo–wetland deposits are composed of the same sediment assemblage (silt and sand) in all units. Change in the hydraulic gradients are harder to define. Certainly, in the lower reaches of discharge systems, hydraulic gradients past and present appear largely unchanged, as judged by the mostly parallel elevation distribution of wetland deposits.

Several advantages of using paleo–wetland deposits as paleoclimatic proxies include the following: (1) they can be ^{14}C dated owing to abundant vascular plant material, (2) numerous exposures allow unit descriptions and ages to be replicated at a given site, and (3) wetlands are common in the Atacama, and records can be easily replicated at numerous localities. Some of the limitations of paleo–wetland deposits are caused by the lack of exposure of the basal sections of deposits and stream erosion. The basal parts of paleo–wetland deposits are often not exposed, and therefore the initiation of water-table rise can be difficult to date. Channel migration of small streams also causes minor unconformities and prevents these deposits from recording short-term climatic fluctuations. Also, when paleo–wetland deposits are confined within stream channels that are the sites of large discharge events, entire units can be eroded. Questions regarding hydrologic response times and the influence of local (geomorphic and/or tectonic) effects on water-table elevation can only be resolved through the comparison of records from several different wetland settings. When deposits of the same age are found at multiple locations, these deposits must be related to regional climatic fluctuations.

Paleo–wetland deposits of similar ages were found within our study areas at Tilomonte, Río Salado, and Río Loa (Fig. 2). Paleo–wetland deposits of similar age have also been described at nearby Quebrada Puripica (Grosjean et al., 1997) and are used in the discussion of past hydrologic changes in the central Atacama Desert. We divided these paleo–wetland deposits in the central Atacama into the following time-stratigraphic units based on >60 AMS (accelerator mass spectrometry) ^{14}C analyses and stratigraphic relationships: unit A (>44 000 ^{14}C yr B.P.), unit B (12 800–8100 ^{14}C yr B.P.), unit C (7400–3000 ^{14}C yr B.P.), and unit D (<2000 ^{14}C yr B.P.).

LABORATORY METHODS

Radiocarbon samples from paleo–wetland deposits were pretreated and cryogenically purified at the University of Arizona's Desert Laboratory, then submitted to the National Science Foundation–University of Arizona Accelerator Mass Spectrometry Laboratory. Samples were first handpicked to isolate the best material for dating and to remove secondary rootlets. Samples were then treated in hot (~70 °C) 2*M* HCl for >1 h to remove all $CaCO_3$, rinsed with deionized water, treated with warm 2% NaOH to separate humates, and then rinsed again with deionized water. The residual fraction after the acid-base pretreatment (A fraction) was separated by filtration, whereas the humates (B fraction) were precipitated by acidification and separated by centrifuging. All samples were combusted at 900 °C with CuO and silver foil, then cryogenically purified.

PALEO–WETLAND DEPOSITS

Dating of Paleo–Wetland Deposits

Various terrestrial organic materials are preserved in the paleo–wetland deposits studied, including organic mats, carbonized wood (oxidized wood retaining primary structure), plant fragments, and organic material encased within tufas. These materials were all ^{14}C dated as a test of their internal consistency. All ^{14}C ages in this section are reported in radiocarbon years before present (1950) (^{14}C yr B.P.), whereas ages in the discussion section have been calibrated (Stuiver and Reimer, 1993; Stuiver et al., 1998) and are presented in calendar years (ka). Radiocarbon ages are listed in Table 1.

Two main sources of potential error in ^{14}C dating of organic material in paleo–wetland deposits are (1) ^{14}C-reservoir effects, which are caused by groundwaters that are depleted in dissolved inorganic $^{14}CO_2$ from either dilution by volcanic CO_2 or water/rock interactions with carbonates, and will yield ages that are too old, and (2) contamination by younger organic matter from secondary vegetation, which will cause ^{14}C ages to be too young. Stream waters in the Atacama are known to be depleted in ^{14}C; water from the Río Loa and Río Tulán contains <25 pmc (percent modern carbon) and <10 pmc, respectively (Fritz et al., 1978; Aravena and Suzuki, 1990). Low ^{14}C concentrations in groundwater, which likely result from the input of volcanic CO_2, will influence the ^{14}C age of vegetation drawing CO_2 directly from groundwater, such as blue-green algae and other aquatic vegetation, but will not affect the ^{14}C age of terrestrial vegetation growing within wetlands that metabolizes atmospheric CO_2. Because bulk organic matter did not yield dates that are consistently older than carbonized wood from terrestrial vegetation within these deposits, we argue that ^{14}C-reservoir effects are either uncommon or negligible.

Secondary rootlets are visible in some organic mats within the deposits studied, particularly near the tops of sections, and were found to be a significant source of contamination in a few samples. Contamination by secondary organic material was found to influence the age of the acid residue fraction (A fraction) within some samples, especially when the total organic carbon content was low and when there were numerous secondary roots. Several samples of bulk organic matter residue from tufas digested in HCl were found

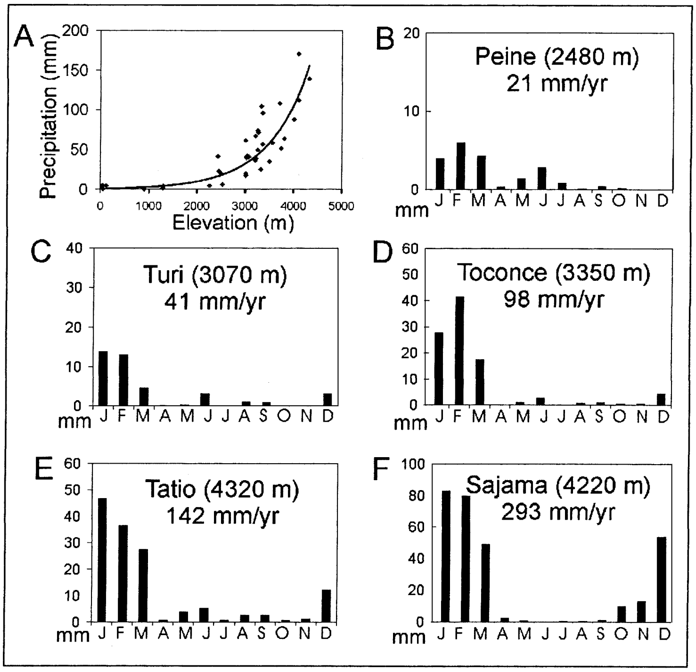

Figure 3. Precipitation in the central Atacama Desert (lat 21°–24°S). (A) Precipitation with elevation. (B–F) Precipitation at selected stations located on Figure 2 (Dirección General de Aguas, no date).

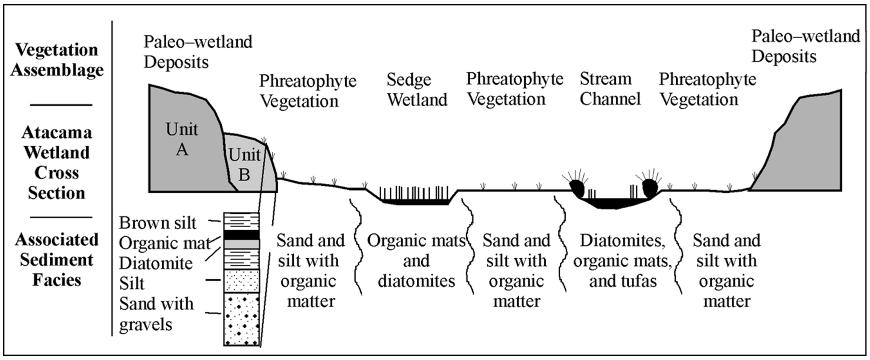

Figure 4. Vegetation and sediment assemblages in modern wetlands.

TABLE 1. RADIOCARBON RESULTS FROM PALEO–WETLAND DEPOSITS

	Lab number	Sample*	Station	Depth (cm)	Material	δ^{13}C† (‰)	^{14}C age (yr B.P.)	s.d.	Cal. age§ (yr B.P.)
Tilomonte									
Unit A	AA37631	AT 375B	34	−550	Organic material	−19.4	37 000	860	
	AA41197	AT 633B	61	−550	Organic material	−22.4	39 900	1200	
Unit B (Tarajne)									
	AA34484	AT 364B	29	−35	Organic material	−22.3	9775	60	11 180
	AA34478	AT 362B	29	−90	Organic material	−16.8	10 330	75	12 190
	AA31200	AT 35A	4	−5	Organic material	−20.9	8115	80	9030
	AA31208	AT 33A	4	−25	Organics in tufa	−25.1	8700	65	9580
	AA32653	AT 31A	3	−25	Organic material	−17.6	8640	65	9550
	AA32652	AT 30B	3	−140	Organic material	−12.6	12 285	80	14 270
	AA34723	AT 29B	3	−165	Organic material	−15.1	12 650	95	14 875
	AA34730	AT 360B	28	−105	Organic material	−13.6	12 820	110	15 440
	AA34848	AT 372A	31	−10	Organics in tufa	(−25.0)	6430	55	7320
	AA34849	AT 371B	31	−50	Organic material	−20.8	10 330	75	12 200
	AA34728	AT 367B	31	−205	Organic material	−22.3	12 740	80	15 360
Unit C (Río Tulán and adjacent areas)									
	AA31204	AT 63A	7	−10	Organics in tufa	−21.8	3140	55	3360
	AA32657	AT 60B	7	−20	Organic material	−23.2	2535	45	2630
	AA31210	AT 61A	7	−35	Root	−22.5	1275	45	1200
	AA32661	AT 58B	7	−60	Carbonized wood	−23.6	3260	50	3470
	AA32651	AT 57A	7	−130	Carbonized wood	−23.5	3805	50	4150
	AA32647	AT 56A	7	−155	Organic material	−24.8	3955	50	4410
	AA32656	AT 55B	7	−180	Organic material	−18.7	3875	50	4240
	AA32658	AT 54B	7	−225	Organic material	−23.4	4875	50	5590
	AA31197	AT 52B	7	−270	Organic material	−21.4	6270	60	7180
	AA32660	AT 51B	7	−325	Organic material	−23.2	7400	60	8180
	AA32655	AT 49B	6	−125	Organic material	−24.3	2460	65	2410
	AA32654	AT 47B	6	−245	Organic material	−23.4	3240	50	3430
	AA31211	AT 81A	10	0	Organics in tufa	−23.2	2840	55	2910
	AA31199	AT 82B	10	−150	Organic material	−24.0	5780	60	6520
	AA37630	AT 379A	34	−450	Organic material	−14.4	7365	60	8170
Unit D (Río Tulán)									
	AA31196	AT 80A	9	−28	Reeds	−23.4	830	45	700
	AA37636	AT 76B	9	−50	Organic material	(−25.0)	330	35	310
	AA31202	AT 75B	9	−120	Organic material	−22.8	6615	55	7480
Río Salado									
Unit A									
	AA32646	AT 111A1	14	−50	Carbonized wood	−24.7	41 400	1700	
	AA32794	AT 111A2	14	−50	Organics in tufa	−25.2	19 240	170	
	AA35154	AT 476A	23	−195	Carbonized wood	−25.0	>44 300		
	AA37632	AT 476B	23	−195	Organic material	−13.4	>49 000		
	AA37634	AT 209B	23	−195	Organic material	−12.3	>49 000		
	AA35158	AT 480A	58	−170	Dispersed organics	−24.5	13 585	80	
Unit C									
	AA38634	AT 503A	18	−105	Carbonized wood	−25.3	4130	40	4670
	AA37638	AT 474B	18	−210	Organic material	−25.0	5900	60	6700
	AA31205	AT 143B	18	−210	Organic material	−24.4	5855	55	6650
	AA31207	AT 133B	17	−20	Organic material	−24.7	4085	50	4550
	AA31206	AT 136B	17	−150	Organic material	−24.8	4285	60	4830
	AA31209	AT 137B	17	−180	Organic material	−24.1	4335	50	4860
	AA32659	AT 138B	17	−270	Organic material	−24.1	4185	55	4730
	AA34479	AT 196A	22	0	Carbonized wood	−23.6	3875	80	4240
	AA34854	AT 188B	21	−30	Organic material	−24.9	3905	45	4320
	AA34855	AT 188A	21	−30	Organic material	−24.7	4015	45	4430
	AA37628	AT 189A	21	−95	Organic material	−25.4	4180	50	4730
	AA37637	AT 185B	21	−220	Organic material	(−25.0)	5900	60	6700
	AA34729	AT 181A	21	−565	Organics in tufa	−16.2	3190	45	3380
	AA41196	AT 513B	60	−550	Organic material	−22.2	6210	60	7090
Modern Organic material									
	AA34724	AT 226B		0	Organic material	−15.1	105	45	25
Río Loa									
Unit A (Chiu Chiu)									
	AA37629	AT 484B	61	−80	Carbonized wood	−24.3	>48 000		
	AA37627	AT 484A	61	−80	Carbonized wood	−24.0	22 470	260	
Unit C (Chiu Chiu)									
	AA31203	AT 125B	16	−40	Organic material	−23.6	3270	50	3470
	AA31195	AT 127B	16	−250	Organic material	−25.2	4295	55	4840
Maria Elana	AA34847	AT 419B	62	−50	Carbonized wood	−24.1	3040	50	3220
	AA34483	AT 418B	62	−95	Carbonized wood	−21.0	3750	40	4090
Unit D	AA35152	AT 422A	63	−215	Carbonized wood	(−25.0)	1395	50	1290
(Quillagua)	AA37633	AT 424A	63	−405	Organic material	−12.8	240	50	215
	AA34851	AT 425A	63	−465	Organic material	−25.0	460	45	510

*An *A* at the end of the sample number represents a radiocarbon age on the acid residue fraction, whereas *B* signifies a humic acid fraction age.
†Values in parentheses indicate an assumed δ^{13}C value.
§Calendar age intercept, or in the case of multiple intercepts, a range midpoint (1σ) was calculated. Calibrated ages are in calendar years before 1950, and were obtained by using Method A of Calib 4.1.2 (INTCAL 98 data set). A Southern Hemisphere correction of 24 yr was applied.

to have secondary rootlet contamination (AT 372A, AT 181A, AT 111A2). This was clearly identified when a matched pair of bulk organic matter and carbonized wood encased within a single tufa sample (AT 111A) returned ages of 19 240 ± 170 ^{14}C yr B.P. for bulk organic matter and 41 400 ± 1700 ^{14}C yr B.P. for carbonized wood. A sample of disseminated carbonized wood (AT 484) also was found to contain secondary contamination when the A fraction yielded an age of 22 470 ^{14}C yr B.P., whereas the B fraction dated to older than 48 000 ^{14}C yr B.P. A small sample of organic material (AT 480A) within a diatomite was found to be contaminated with younger organic material when the A fraction yielded an age of 13 585 ± 80 ^{14}C yr B.P. and carbonized wood in an organic mat from a different location of the same unit yielded infinite ^{14}C ages (AT 476A, AT 476B, AT 209B).

To minimize contamination by younger particulate organic material, we focused on dating the humate fraction (B fraction) of most samples (Quade et al., 1998). Humate fractions were deemed to be reliable for dating in this study because (1) few stratigraphic violations were found when carbonized wood and organic mat humates were dated within one section (e.g., Tilomonte, sta. 7), (2) humate and residue fractions of organic mats yielded the same age (AT 188A and AT 188B), and (3) modern humates from an organic mat yielded an age of 105 ^{14}C yr B.P. In some cases, however, humate fractions of organic mats were slightly contaminated by younger organic matter (AT 60B). Radiocarbon ages on all materials near the top of sections, except for well-preserved carbonized wood, should thus be viewed as minimum ages because of increased potential for rootlet contamination.

Tilomonte Springs

Tilomonte Springs consists of a series of springs and spring-fed streams with wetlands near the base of the Andes between 2400 and 2600 m (Fig. 5). Río Tulán, which bisects Tilomonte, is a deeply incised (10–15 m) perennial stream that has a drainage area of ~400 km² and a catchment extending up to 4000 m. Intermittent streams located to the north and south of Río Tulán have drainage areas of <10 km², are not as incised, and generally have catchments below 3000 m. Within many of these intermittent-stream channels, groundwater surfaces for short distances (<50 m). Travertine and paleo–wetland deposits at Tilomonte record a long history of groundwater discharge and water-table fluctuations. Travertine deposits, likely middle to late Pleistocene in age, are generally <1 m thick and form a surface cap over a large area of Tilomonte. Paleo–wetland deposits, composed of units A, B, C, and D, are located north of Río Tulán at Tarajne between 2550 and 2600 m, within and just to the north of the incised channel of Río Tulán between 2500 and 2650 m, and south of Río Tulán between 2500 and 2550 m (Fig. 5).

Unit A

Paleo–wetland deposits that are beyond the range of ^{14}C analysis (unit A) are located to the south of Río Tulán, between 2500 and 2550 m (Fig. 5). The deposits generally consist of a sequence of diatomite and fine-grained sediments in the basal part (lower 2 m), whereas the upper 3 to 5 m is composed of silty sand. The deposits are currently close to the modern water table and are therefore heavily cemented with secondary salts and support large areas of phreatophyte vegetation, which hindered attempts to map and collect samples. Two ^{14}C ages, from station 34 (AT 375B) and station 61 (AT 633B), both from a depth of −550 cm, yielded ages of 37 000 ± 860 ^{14}C yr B.P. and 39 900 ± 1200 ^{14}C yr B.P. A sample from station 34 at −450 cm depth, however, yielded an age of 7365 ± 60 ^{14}C yr B.P. Although no obvious unconformity was visible in the field, this sample may be from the base of the middle Holocene wetland unit (unit C, described subsequently).

Unit B

Paleo–wetland deposits dating to the late glacial to early Holocene (unit B) are located at Tarajne (Figs. 5 and 6). Radiocarbon ages from unit B range from 12 820 ^{14}C yr B.P. to 8115 ^{14}C yr B.P. A 2.8-m-thick section (sta. 28), located 2 km north of Río Tulán, contains a series of thin (2–5 cm) diatomites and tufa interbedded with fine sand and silt (Fig. 7). This section contained one thin (2 cm) organic mat at a depth of −110 cm (AT 360B) that yielded an age of 12 820 ± 110 ^{14}C yr B.P. Below this mat, deposits 1.7 m thick and containing several diatomites and tufas indicate that the water table was high in this region prior to 12 800 ^{14}C yr B.P. A section located ~1.6 km north of Río Tulán (sta. 29) contains a 55-cm-thick organic mat resting upon a white diatomite (Fig. 7). Radiocarbon ages from the bottom and top of this organic mat yielded ages of 10 330 ± 75 ^{14}C yr B.P. (AT 362B) and 9775 ± 60 ^{14}C yr B.P. (AT 364B), respectively. The presence of a thick (60 cm) diatomite below the organic mat identifies a high water table in this area well before the formation of the organic mat.

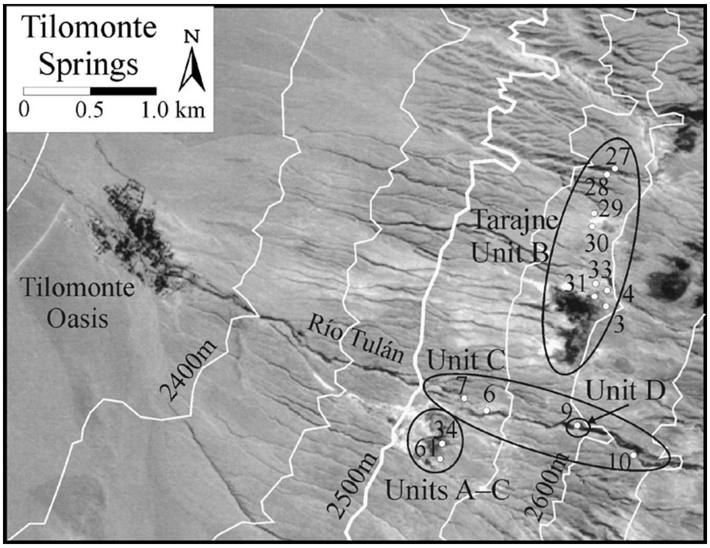

Figure 5. Aerial photograph of Tilomonte Springs. Tarajne (unit B) paleo–wetland deposits are located to the north of Río Tulán between 2550 and 2600 m. Paleo–wetland deposits (units A–C) are visible to the south of Río Tulán, just above 2500 m. Unit C deposits are also located along and just to the north of Río Tulán. Unit D is only present at one location along Río Tulán. Circles and associated station numbers represent mapped sections.

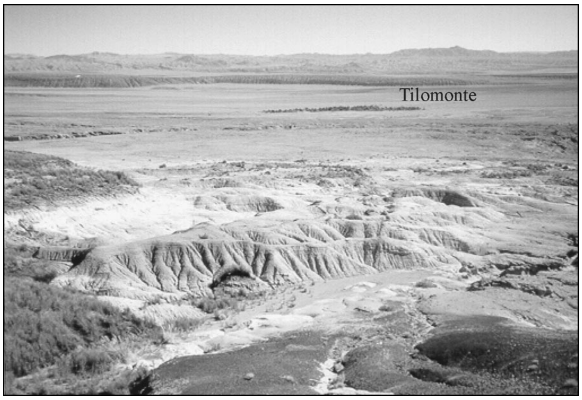

Figure 6. View of unit B paleo–wetland deposits at Tarajne (sta. 27 and sta. 28) from the north. Tilomonte oasis (<1 km²) is observable in the background. Prominent dark ridge in background is the midden site Lomas de Tilocalar (Betancourt et al., 2000; Latorre et al., 2002).

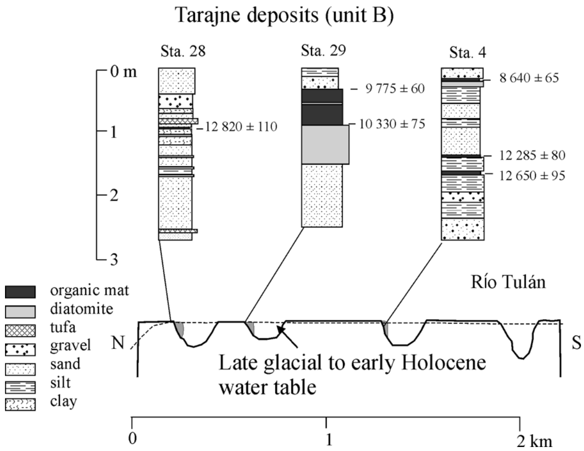

Figure 7. Cross section of unit B deposits at Tarajne, 2580 m. Ages in ^{14}C yr B.P.

Figure 8. View of unit C deposits situated 11 m above the modern stream level along Río Tulán.

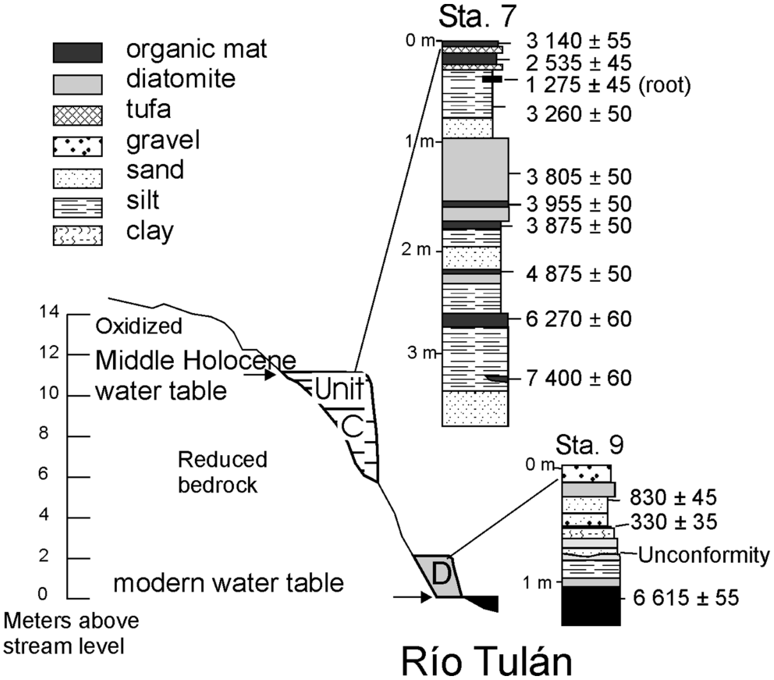

Figure 9. Cross section of Río Tulán and relationship between unit C and unit D deposits. Ages in ^{14}C yr B.P.

Three sections located ~1 km north of Río Tulán were mapped and ^{14}C dated. A 90-cm-thick section (sta. 4) contains sand and gravel in the bottom 50 cm and organic mats, silt, and tufa in the upper 40 cm. An organic mat from a depth of −25 cm (AT 33A) yielded an age of 8700 ± 65 ^{14}C yr B.P., and an organic mat at −5 cm (AT 35A) gave an age of 8115 ± 80 ^{14}C yr B.P. Three organic mats in station 3, just south of station 4, yielded ages of 12 650 ± 95 ^{14}C yr B.P. (AT 29B) at −165 cm, 12 285 ± 80 ^{14}C yr B.P. (AT 30B) at −140 cm, and 8640 ± 65 (AT 31A) at −25 cm (Fig. 7). A section (at sta. 31) ~100 m downstream from station 4 yielded ages of 12 740 ± 80 (AT 367B) at −205 cm, 10 330 ± 75 (AT 371B) at −50 cm, and 6430 ± 55 (AT 372A) at −10 cm. The ^{14}C age on the upper organic mat was on residual organic matter from within a tufa and is likely contaminated by young rootlets. Modern *Tessaria* roots were observed in the top of this section.

Unit C

Paleo–wetland deposits dating to the middle Holocene (unit C) are located to the north of Río Tulán, within the Río Tulán stream channel, between 2525 m and 2625 m, and just to the south at ~2500 m (Fig. 5). These deposits date from ca. 7400 ^{14}C yr B.P. at the base of the unit to ca. 3000 ^{14}C yr B.P. The top of unit C deposits along the Río Tulán steam channel are ~11 m above the modern stream level (Figs. 8 and 9). Above ~2550 m, Río Tulán is incised >15 m, and only resistant parts of unit C deposits remain, forming a conspicuous ledge. The former location of deposits, however, is marked by a reduced weathering rind on the volcanic bedrock up to +11 m along Río Tulán, whereas above this height, the bedrock is oxidized. Below ~2550 m, the bedrock channel is less incised, and unit C deposits are located above the bedrock channel (Fig. 8). Deposits in this area are extremely well preserved even though they are quite loose and easily eroded.

Our best-dated section from these deposits is station 7 located at 2530 m (Figs. 5 and 9). Ten AMS radiocarbon dates on organic mat humates, carbonized wood, and organic material encased within tufas securely date this profile to the middle Holocene, from 7400 ± 60 ^{14}C yr B.P. (AT 51B) to 3140 ± 55 ^{14}C yr B.P. (AT 63A). This section grades from coarse sand and gravel near the base to silt and fine sand, organic mats, diatomite, siliceous sinter, and tufa in the upper part of the section (Fig. 9). Mesquite (*Prosopis*) roots in the upper 20 cm of the section (AT 61A) yielded an age of 1275 ± 45 ^{14}C yr B.P. This age represents a minimum age for the drop of the water table because mesquites typically grow only where the water table is several meters below the surface. Some of the paleo–wetland deposits to the south of Río Tulán are also probably of middle Holocene age. These deposits can be traced laterally from unit C deposits along Río Tulán.

Unit D

Paleo–wetland deposits dating to younger than 2000 ^{14}C yr B.P. (unit D) were found at only one location at Tilomonte. A section (sta. 9) located ~2 m above the modern stream level of Río Tulán contains a thick (>40 cm) organic mat at the base (AT 75B), which lies below a clear unconformity. Humates from this organic mat returned an age of 6615 ± 55 ^{14}C yr B.P. (Fig. 9). Humates from an organic mat at −50 cm (AT 76B), above the unconformity, yielded an age of 330 ± 35 ^{14}C yr B.P., and buried reeds (AT 80A) from a depth of −28 cm yielded an age of 830 ± 45 ^{14}C yr B.P. The age on the buried reeds is thought to be the most reliable age and provides a minimum age for the termination of ~11 m of incision that occurred in Río Tulán after the deposition of unit C. The age of 330 ± 35 ^{14}C yr B.P. is too young, possibly owing to the presence of young humates, which also may influence the age of 6615 ± 55 ^{14}C yr B.P.

Summary

Paleo–wetland deposits at Tilomonte provide a detailed record of water-table changes

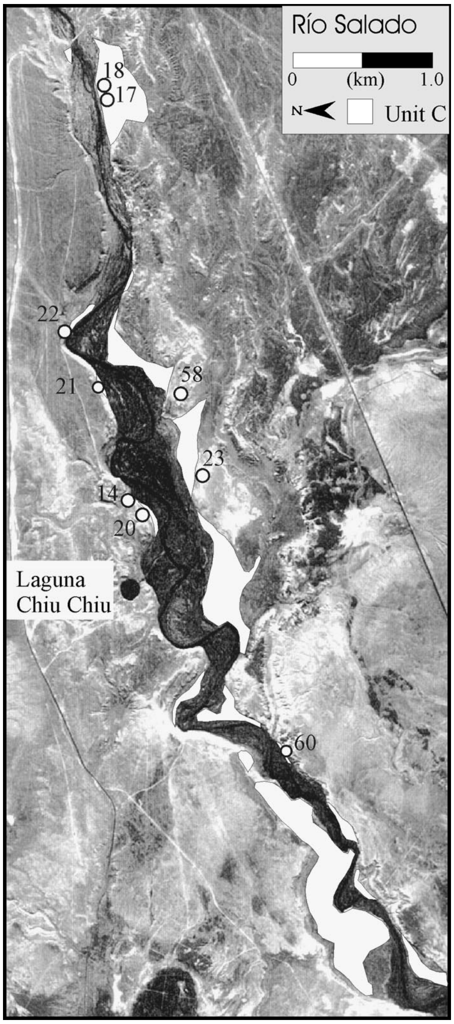

Figure 10. Aerial photograph of Río Salado identifying extent of unit C deposits and station locations.

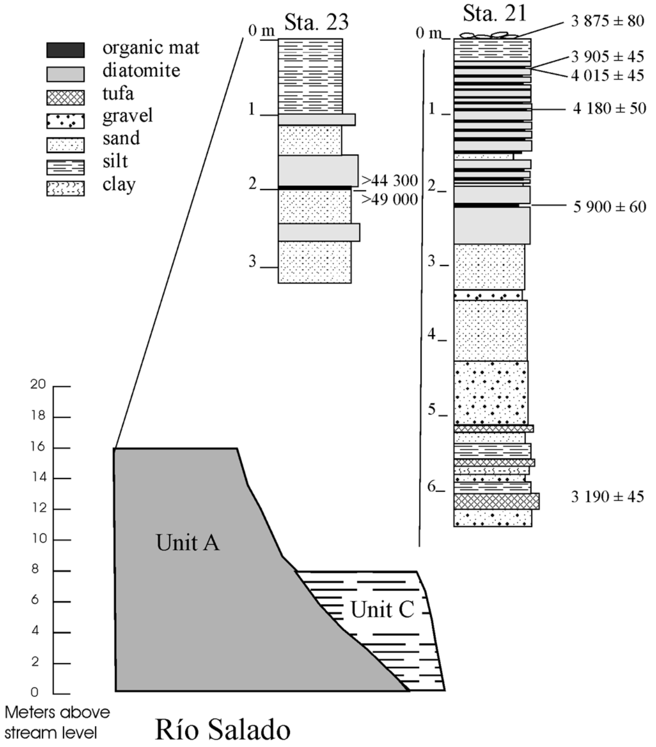

Figure 11. Cross-sectional relationship of units A and C on Río Salado. Ages in ^{14}C yr B.P.

over the past 13.0 ^{14}C ka. The water table was highest between >12.8 and 8.1 ^{14}C ka when the area of Tarajne supported perennial wetlands. Between 8.1 and >7.4 ^{14}C ka, the water table dropped significantly. By 7.4 ^{14}C ka, however, channel incision had ended and sediment was aggrading along Río Tulán. Between 7.4 and 3.0 ^{14}C ka, the water table along Río Tulán was 8–11 m above the modern stream level. Sometime after ca. 3.0 ^{14}C ka and before 0.8 ^{14}C ka, Río Tulán incised through 11 m of deposits to its modern level. Unit D deposits, dated to ca. 0.8 ^{14}C ka, identify a minor increase of ~2 m in the water table at this time.

Río Salado

The Río Salado is a perennial stream located ~150 km north of Tilomonte (Fig. 2). The Río Salado originates at >4000 m in the Andes and becomes perennial at ~3500 m. At the intersection with the Calama depositional basin (~2500 m), it switches from a bedrock-incised channel with a steep longitudinal gradient to a low-energy meandering stream that intersects the water table. Both modern and paleo–wetland deposits begin at this intersection and continue beyond the junction of the Río Salado and Río Loa (Fig. 2). Our study area consists of an ~8 km reach of the Río Salado from the beginning of the modern wetland deposits to just upstream of the Río Loa confluence (Fig. 10). Two paleo–wetland units, units A and C, occur as inset terraces that are up to +20 m and +10 m above the modern stream level, respectively (Fig. 11).

Unit A

Unit A deposits, >44 000 ^{14}C yr B.P., are located between ~10 and 20 m above the modern stream level (Fig. 11). Unit A deposits are not all contemporaneous in age, but were deposited during several separate episodes of wetland accumulation likely spanning the middle and late Pleistocene. It is possible to separate at least three individual deposits by the presence of major unconformities and included distinctive beds at some locations. Because most of these deposits are similar in appearance and beyond the age of ^{14}C dating, it was not possible to further resolve them in the field. On the north bank, unit A is heavily cemented with secondary salts (gypsum and halite) and forms a flat surface clearly visible in aerial photographs (Fig. 10). On the south bank, across from Laguna Chiu Chiu and to the east of this location, the youngest deposits of unit A are present (sta. 23 and sta. 58). These deposits are identifiable by a conspicuous cap of red silt and are not as heavily cemented by secondary salts as older unit A deposits. All deposits, however, are beyond the range of ^{14}C dating (AT 476A, AT 476B, AT 209B). Young ages of 13 585 ± 80 ^{14}C yr B.P. (AT 480A) and 19 240 ± 170 ^{14}C yr B.P. (AT 111 A2) are the result of contamination by secondary vegetation.

Unit C

Middle Holocene unit C deposits are almost continuous along the Río Salado for the entire range of our study area (Fig. 10). The top of these deposits ranges between 6 and 10 m above the modern stream level. Unit C deposits are inset against older (unit A) deposits (Fig. 12). At most locations, the middle Holocene sequence consists of 3–4 m of sand and gravel at the base of deposits capped by a pronounced 2–3 m section of finely bedded (2–5

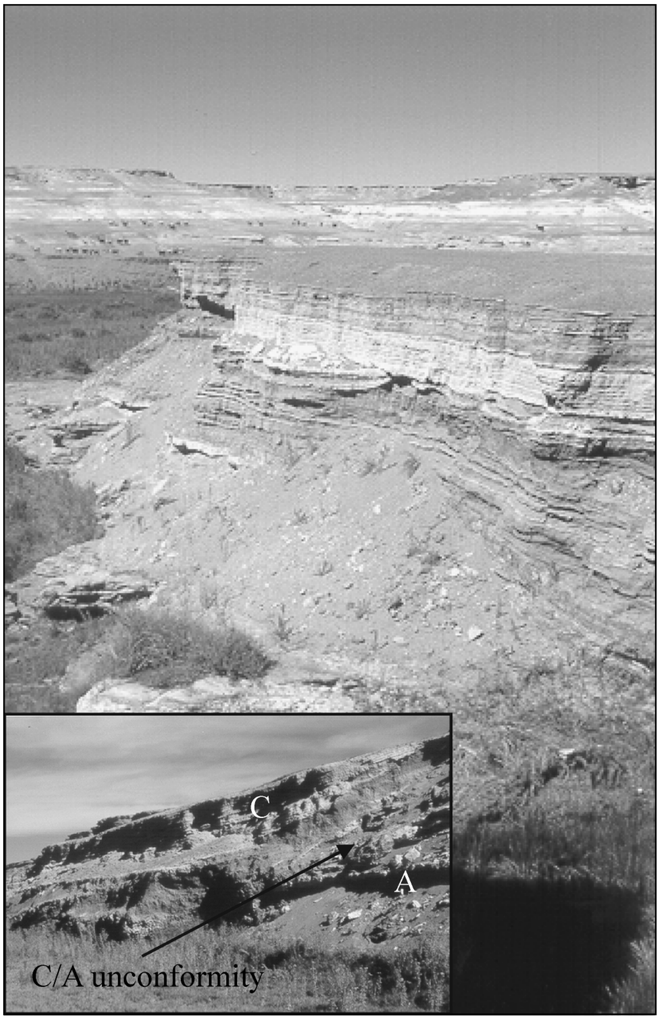

Figure 12. Photograph of unit C deposits (foreground) ~8 m thick, with fine-bedded diatomite (2–5 cm) and organic mats in upper ~3 m. Photograph in lower left displays the inset relationship of unit C against unit A deposits.

cm) diatomites and organic mats at the top of the section (Figs. 11 and 12).

Unit C deposits on the Río Salado date from ca. 6210–4000 ^{14}C yr B.P. (Fig. 11) (Table 1). The top of this unit is well dated by a matched pair of humate and residual fractions from an organic mat at a depth of −30 cm and a sample of carbonized wood on top of the section (sta. 21) buried by rockfall debris. The humate and residual fraction of the organic mat yielded ages of 3905 ± 45 (AT 188B) and 4015 ± 45 (AT 188A) ^{14}C yr B.P., and the carbonized wood (AT 196A) returned an age of 3875 ± 80 ^{14}C yr B.P. An organic mat (AT 185B) near the base of the finely bedded diatomite section yielded an age of 5900 ± 60 ^{14}C yr B.P. at station 21. This age agrees well with a date of 5855 ± 55 ^{14}C yr B.P. on an organic mat (AT 143B) at the base of the finely bedded diatomite at station 18. An attempt to date organic matter encased within tufa at the base of station 21 (AT 181A) was unsuccessful; the ^{14}C age of 3190 ± 45 ^{14}C yr B.P. is much younger than organic mats higher in the section, indicating contamination by secondary organic matter. An organic mat (At 513B) at the base of station 60 yielded an age of 6210 ± 60 ^{14}C yr B.P.

Summary

Paleo–wetland deposits along Río Salado identify two periods of high water tables. The oldest of these periods is represented by the highest terrace (unit A) and occurred sometime prior to 44.0 ^{14}C ka. No evidence of late glacial to early Holocene paleo–wetland deposits (unit B) was found at Río Salado. These deposits may have been eroded, have not yet been located, or are buried beneath unit C deposits. Sometime prior to 6.2 ^{14}C ka, the Río Salado incised to at least its modern level. Unit C deposits are extensive and are associated with a water table that was ~8 m higher than the modern level. The beginning of aggradation of unit C occurred at ca. 6.2 ^{14}C ka. The upper 2–3 m of this unit consists of a section of finely bedded organic mats and diatomite that was deposited between 5.9 and 4.0 ^{14}C ka (Fig. 11). The nature and age of this upper part of the unit C deposits clearly show that the water table was stable and at a significantly higher level during this period. Sometime after 4.0 ^{14}C ka, the Río Salado incised through unit C deposits to at least its modern level.

Río Loa

The Río Loa is the only perennial stream in this region of the Atacama that discharges into the Pacific Ocean. We sampled paleo–wetland deposits at three locations: (1) at Chiu Chiu (lat 22°0′S, long 68°39′W), (2) ~100 km downstream from Chiu Chiu near Maria Elena (lat 22°16′S, long 69°33′W), and (3) at Quillagua (lat 21°37′S, long 69°32′W), ~170 km downstream from Chiu Chiu (Fig. 2). Paleo–wetland deposits from units A, C, and D are present at these locations.

Unit A

Unit A deposits are present on the Río Loa at Chiu Chiu (Fig. 13A). At this location, a 1-m-thick exposure of unit A deposits, ~19 m above the modern stream level, consists of white diatomite, tufa, and a thin brown silt with carbonized wood. A matched pair of humate and residual radiocarbon ages on this disseminated wood (AT 484) yielded ages of 22 470 ± 260 ^{14}C yr B.P. for the residual fraction and older than 48 000 ^{14}C yr B.P. for the humate fraction. The younger age on the residual fraction is thought to reflect contamination by secondary organic matter.

Unit C

Unit C deposits are located on the Río Loa at both the Chiu Chiu and Maria Elena locations (Fig. 13, A and B). At Chiu Chiu, unit C is ~11 m above the modern stream level and contains a sequence of organic mats, tufa, silt, and sand. An organic mat at a depth of −250 cm (AT 127B) yielded an age of 4295 ± 55 ^{14}C yr B.P. on the humate fraction, and humates from an organic mat at −40 cm (AT 125B) gave an age of 3270 ± 50 ^{14}C yr B.P. (Fig. 13A). At Maria Elena, the top of unit C is ~5 m above the modern stream level and is composed mostly of alluvial sediment, with one 10-cm-thick diatomite near the top of the

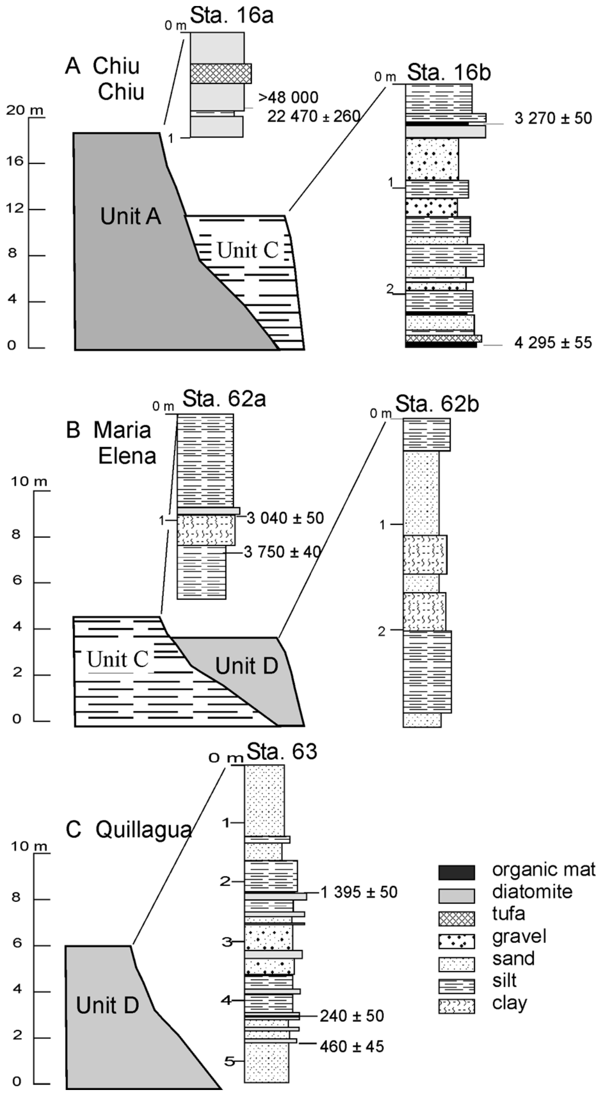

Figure 13. Cross-sectional relationships of paleo–wetland units on the Río Loa at (A) Chiu Chiu, (B) Maria Elena, and (C) Quillagua. Ages in ^{14}C yr B.P.

section. Two lenses of carbonized wood at depths of −95 cm (AT 418B) and −50 cm (AT 419B) yielded ages of 3750 ± 40 and 3040 ± 50 ^{14}C yr B.P. on humate fractions (Fig. 13B).

Unit D

Unit D deposits are present at both Maria Elena and downstream at Quillagua (Fig. 13, B and C). At Maria Elena, this unit is inset against unit C deposits and is ~4 m above the modern stream level (Fig. 13B). This unit is composed entirely of alluvial sediment and contains no organic mats, tufa, or diatomite. No material was found in this unit to radiocarbon date. At Quillagua (Fig. 13C), unit D is ~6 m above the modern stream level and contains diatomite and organic mats, especially in the basal 4 m. The upper 2 m of the deposit is bedded sand and silt. The residual fraction of organic mats at −460 cm (AT 425A) and −410 cm (AT 424A) yielded ages of 460 ± 45 ^{14}C yr B.P. and 240 ± 50 ^{14}C yr B.P. A radiocarbon date on carbonized wood at −215 cm (AT 422A) yielded an age of 1395 ± 50 ^{14}C yr B.P. The age on carbonized wood is considered the most reliable age from this section. Young ages on the residual fractions of organic mats may be the result of contamination by secondary organic matter.

Summary

Paleo–wetland deposits on the Río Loa identify three episodes of elevated water tables. Unit A deposits represent a period >44.0 ^{14}C ka when the water table was 19 m higher than today at the Chiu Chiu locality. A second episode of high water tables occurred during the middle Holocene, between >4.2 and 3.0 ^{14}C ka, as evidenced by unit C deposits 11 m above the modern water level at Chiu Chiu and 5 m above modern at Maria Elena. Only the upper sections of these deposits are exposed, and therefore the beginning age of aggradation of this unit is unknown. A final episode of high water tables, recorded as unit D, occurred during the late Holocene and is documented by deposits 6 m above the modern water level at Quillagua and 4 m above the modern water level at Maria Elena. The age of unit D is not well determined, but the age of 1395 ± 50 ^{14}C yr B.P. from the top of the Quillagua section provides an age for the end of aggradation of this unit.

Quebrada Puripica

Quebrada Puripica is a perennial stream located between our study areas at Tilomonte and Ríos Loa and Salado (Fig. 2). Quebrada Puripica is a typical Andean stream with a deeply incised (~30 m) channel and limited modern discharge. Holocene deposits at the intersection of Quebrada Puripica and the tributary Quebrada Seca (~3450 m) date between 6200 and 3100 ^{14}C yr B.P. (Grosjean et al., 1997), the same age as unit C deposits presented in this study. These deposits, however, were originally interpreted by Grosjean et al. (1997) as lacustrine and wetland deposits that formed as a result of episodic damming by debris flows from Quebrada Seca, a deeply entrenched tributary. Grosjean et al. (1997) argued that the debris flows dammed Quebrada Puripica, creating temporary lakes and wetlands upstream from the Puripica/Seca junction. Further examination of this area (Rech and Pigati, 2000), however, identified the presence of Holocene wetland deposits over a 6 km reach of the stream, both upstream and downstream from the confluence with Quebrada Seca. Therefore, we believe the Puripica deposits are paleo–wetland deposits akin to the ones presented in this study.

SYNTHESIS OF RECORDS

The combined paleo–wetland records from Tilomonte, Río Salado, Río Loa, and Quebrada Puripica chronicle a coherent story of water-table fluctuations in the central Atacama (Fig. 14). Water tables were highest before 44.0 ^{14}C ka and are identified by deposits of unit A that are up to 20 m above the modern water level on the Río Salado and Río Loa. No paleo–wetland deposits dating to the LGM

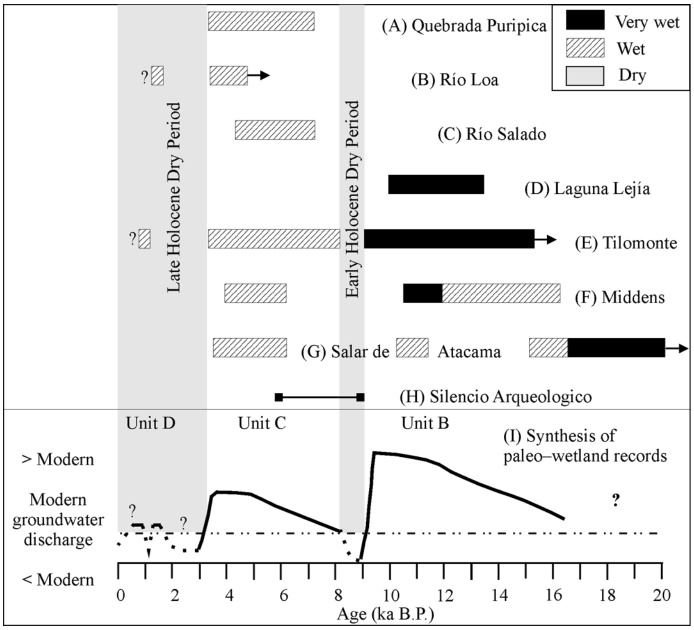

Figure 14. Paleoclimatic records from the central Atacama, lat 22°–24°S: (A) Grosjean et al. (1997); (B and C) this study; (D) Grosjean (1994), Geyh et al. (1999); (E) this study; (F) Betancourt et al. (2000); (G) Bobst et al. (2001); (H) Grosjean et al. (1997). (I) Synthesis of wetland records from this study based on age and depth of deposits and the stratigraphic relationships of units.

were found in the study area. The absence of deposits of LGM age could be the result either of erosion or of nondeposition due to low water tables at this time. A second period of high water tables is associated with unit B deposits at Tilomonte and happened during the late glacial to early Holocene. These deposits date between >12.8 and 8.1 ^{14}C ka (>15.4–9.0 ka). This is the only time when water tables were high enough to support extensive wetlands at Tarajne. Late glacial to early Holocene deposits (unit B) were not found along Río Tulán at Tilomonte or along Ríos Salado and Loa. The absence of such deposits may be the result of subsequent erosion in streams with periodic large discharges.

The end of the early Holocene was marked by a period between ca. 8.1 and 7.4 ^{14}C ka (9.0–8.2 ka) when water tables dropped significantly and streams incised. The inset relationship of the middle Holocene unit, unit C, on Río Salado and Río Tulán indicates that streams incised to approximately modern levels prior to the deposition of unit C. After this period of incision, by 7.4 ^{14}C ka, water tables began to rise. Unit C deposits at Río Tulán (+11 m), Río Salado (+8 m), Río Loa (+6 to +11 m), and Quebrada Puripica (between +5 and +32 m) all identify significantly higher water tables during the middle Holocene. Unit C deposits range in age from 7.4 to ca. 3.0 ^{14}C ka (8.2–3.1 ka) at Tilomonte, 6.2–4.0 ^{14}C ka (7.1–4.3 ka) at Río Salado, >4.3–3.0 ^{14}C ka (>4.9–3.5 ka) at Río Loa, and 6.2–3.1 ^{14}C ka (7.1–3.3 ka) at Quebrada Puripica. Basal parts of unit C deposits are not exposed on Río Loa. The end of aggradation of unit C deposits on Río Salado, which is well dated with carbonized wood on top of the deposit dating to 3875 ± 80 ^{14}C yr B.P. (4.3 ka), preceded the end of deposition of unit C at Río Tulán, Río Loa, and Quebrada Puripica by ~1000 yr. The reason for this discrepancy between records is unknown, but may be due to differences in the groundwater flow paths and lag times of these distinct hydrologic systems.

Water tables fell significantly sometime between ca. 3.0 ^{14}C ka (3.1 ka) (perhaps as early as 4.0 ^{14}C ka [4.3 ka] at Río Salado) and ca. 0.8 ^{14}C ka (0.7 ka). During this period, the Río Tulán, Río Salado, Río Loa, and Quebrada Puripica all incised through unit C deposits. This period of erosion ended sometime prior to 0.8 ^{14}C ka (0.7 ka) at Río Tulán and prior to 1.4 ^{14}C ka (1.3 ka) on Río Loa at Quillagua. At other locations, the age for the end of incision of unit C deposits is not well determined. Unit D deposits at Río Tulán and Rio Loa are not well dated and represent minor water-table changes. At this point, it is unclear whether water-table fluctuations associated with unit D are contemporaneous and whether they represent regional or local processes.

Implication of Water-Table Change

The synthesis of paleo–wetland records from deposits at Tilomonte, Río Salado, Río Loa, and Quebrada Puripica provide a detailed history of hydrologic changes in the central Atacama. Increased water-table heights at these locations reflect enhanced groundwater discharge, which can be supported only by higher recharge and precipitation in the High Andes. Furthermore, the general concordance of records from different parts of the regional hydrologic system—including groundwater-fed Andean streams (Quebrada Puripica, Río Tulán), point-source springs (Tarajne), and water tables in the Calama basin (Río Loa, Río Salado)—suggests a relatively synchronous response to changes in regional recharge, notwithstanding major differences in size, gradients, and location of the hydrologic systems with respect to the recharge area. We therefore argue that this regional control must be climate and that the response times of these separate hydrologic systems are short.

DISCUSSION

Central Atacama Records

Evidence from other paleoclimatic proxy records in the central Atacama (lat 22°–24°S) comes primarily from rodent middens (Betancourt et al., 2000; Latorre et al., 2002), small Altiplano lakes (Grosjean, 1994; Grosjean et al., 1995, 2000; Valero-Garcés et al., 1996; Geyh et al., 1999), sediment cores from the Salar de Atacama (Bobst et al., 2001), and archaeological site density over time (Lynch and Stevenson, 1992; Grosjean and Núñez, 1994; Grosjean et al., 1997) (Fig. 14).

Fossil rodent middens located along the lower elevation limits of vascular plants in the central Atacama (~2700 m) identify periods of vegetation encroachment into the hyperarid core of the Atacama Desert that are thought to result from increased precipitation (Betancourt et al., 2000; Latorre et al., 2002). High grass concentrations and species abundance in middens reflect wetter conditions from 16.2 to 10.5 ka and slightly wetter conditions from 7. to 3.9 ka. The absence of middens between 35 and 22 ka and the low grass and species abundance in a midden dated at 22 ka is thought to be indicative of a dry climate.

Lakes on the Chilean Altiplano and saline salt pans from the Salar de Atacama provide additional evidence of regional changes in the hydrologic budget of the central Atacama. Lakes on the Chilean Altiplano record a wet late glacial to early Holocene, hyperaridity during the middle Holocene, and a return to modern climatic conditions during the late Holocene (Grosjean, 1994; Grosjean et al., 1995, 2000; Valero-Garcés et al., 1996; Geyh et al., 1999). Terrestrial macrofossils, archaeological charcoal, and peat provide the most reliable ^{14}C results for lake highstands. Ten ^{14}C ages on terrestrial organic samples from six lakes and marshes between lat 23° and 25°S identify a lake-level rise between 15.5 and 14.0 ka, a lake-level maximum from 12.5–10.2 ka, and a lake-level fall between 9.3 and 8.9 ka (Geyh et al., 1999). The period of high lake levels correlates well with the age of unit B from Tilomonte, dating between >15.4 and 9.0 ka.

The evidence for middle Holocene aridity from small lake records, however, is at odds with our data from paleo–wetland deposits. Evidence for middle Holocene aridity in the region comes primarily from Laguna Miscanti, where diatomaceous aragonite mud with gypsum—present in cores from a depth of ~3.75–2.0 m (Grosjean et al., 2000) and between 2.92 and 1.83 m (Valero-Garcés et al., 1996)—is thought to represent lake desiccation (Valero-Garcés et al., 1996; Grosjean et al., 2000). The chronology from Laguna Miscanti, however, involves significant and variable ^{14}C-reservoir corrections ranging between 1000 and 4000 yr, which makes the age of this record uncertain (Valero-Garcés et al., 1996; Grosjean et al., 2000). Paleo–wetland deposits from Quebrada Puripica were also reported to indicate middle Holocene aridity and to have been due to side-canyon damming by debris flows (Grosjean et al., 1997); however, we disagree with this interpretation (Rech and Pigati, 2000).

Cores from the Salar de Atacama, a predominately groundwater-fed closed basin at the base of the Andes that receives discharge from Quebrada Puripica and our study area of Tilomonte (Fig. 2), contain evidence of several periods of saline lakes in the salar over the past 100 ka (Bobst et al., 2001). The latter part of this record, which overlaps with the wetland deposits presented here, indicates a perennial saline lake between 26.7 and 16.5 ka, expanded saline mudflats from 16.5 to 15.3 ka, and shallow saline lakes from 11.4 to 10.2 ka and from 6.2 to 3.5 ka. The presence of expanded saline mudflats from 16.5 to 15.3 ka, indicative of greater surface discharge into the salar, and of shallow to ephemeral saline lakes from 11.4 to 10.2 ka and from 6.2 to 3.5 ka agrees well with evidence of higher regional water tables indicated by wetland deposits during these periods. The identification of a wet LGM, however, is at odds with the wetland records. The discrepancy between records may be due to (1) temperature effects on the large (~3000 km^2), shallow lake, (2) overflow from closed basins to the south (Bobst et al., 2001), or (3) gaps in the wetland records.

The clustering of archaeological sites in the central Atacama during the early and late Holocene—combined with the general lack of archaeological sites at low elevations during the middle Holocene (9.0–5.7 ka, termed the *Silencio Arqueologico*)—and the site expansion during the late Holocene have been interpreted climatically (Grosjean and Núñez, 1994, Grosjean et al., 1997). Although some parts of this record may be due to climate change, such as the beginning of the *Silencio Arqueologico*, cultural innovations such as animal domestication and associated population expansions preclude this record from solely representing climate change in the central Atacama.

Bolivian and Peruvian Altiplano

Evidence for past hydrologic budgets from the neighboring Altiplano of Bolivia and Peru comes mostly from the Lake Titicaca–Salar de Coipasa–Salar de Uyuni system and smaller lakes to the north. The Lake Titicaca–Salar de Coipasa–Salar de Uyuni system, located ~200–800 km north of the central Atacama (Fig. 1), is a series of interconnected basins that at times coalesced into a series of lakes covering >60 000 km^2 (Wirrmann and Mourguiart, 1995). Paleorecords from this lake system have been used to represent regional and continental climatic trends (Sylvestre et al., 1999; Baker et al., 2001a).

Lake Titicaca is a deep, freshwater lake located on the Altiplano between 16° and 17.5°S. Lake Titicaca currently overflows through the Río Desaguadero spillway and feeds a series of connected basins including Lago Poopó, Salar de Coipasa, and Salar de Uyuni. Sediment cores have been collected and analyzed from both deep (Baker et al., 2001a) and shallow areas (Wirrmann and de Oliveira Almeida, 1987; Ybert, 1992; Wirrmann and Mourguiart, 1995; Cross et al., 2000) of the lake. Lake-level proxies—including benthic, planktonic, and saline diatom abundance, weight percent of $CaCO_3$, and $\delta^{13}C$ values of organic matter—from a series of cores between 89 and 250 m depth from Lake Titicaca provide a 25 k.y. record of lake-level fluctuations (Baker et al., 2001a). Lake Titicaca was deep and overflowing from 25 to 15, from 13 to 11.5, from 10 to 8.5 ka, and during multiple short periods during the late Holocene (Abbott et al., 1997), including today. The lake was below the overflow level from 15 to 13, from 11.5 to 10, and from 8.5 to 5 ka; the lake level was at least 85 m below the modern level between 6 and 5 ka (Cross et al., 2000; Baker et al., 2001a). Algae percentage from core TD (Ybert, 1992; Sylvestre et al., 1999) suggests that this lake-level drop began prior to 10.8 ka, and algae percentage from core TD1 suggests a lake-level drop prior to 7.8 ka.

Chronologies of lake highstands from the evaporite lakes of Salar de Coipasa–Salar de Uyuni and Lake Poopó, at the southern end of the Lake Titicaca system, have been reconstructed from $^{230}Th/^{234}U$ and ^{14}C ages on calcium carbonate from tufa and mollusks (Servant and Fontes, 1978; Rondeau, 1990; Wirrmann and Mourguiart, 1995; Servant et al., 1995; Clayton and Clapperton, 1997; Sylvestre et al., 1999) and from a sediment core from Salar de Uyuni (Baker et al., 2001b). The older shoreline tufas from these evaporite lake basins date between 45 and 35 ka with $^{230}Th/^{234}U$ ages (Rondeau, 1990) and at ca. 38 ka with ^{14}C ages (Wirrmann and Mourguiart, 1995); the tufas are argued to represent the Minchin highstand. Paleo-Lake Tauca of late glacial age was dated at 19 to 14 ka, and its maximum lake levels were dated at 15.5 to 14 ka by Sylvestre et al. (1999); the lake's age was dated at ca. 16 to ca. 13.6 ka, and its maximum levels were dated at ca. 15.5 to ca. 13.6 ka by Clayton and Clapperton (1997) (Fig. 15). A minor lake phase, Coipasa, has been placed from 10.5 to 9.5 ka on the basis of ^{14}C ages of stromatolitic crusts (Sylvestre et al., 1999). Intercalated mud with diatoms and salt deposits from the Salar de Uyuni core (Baker et al., 2001b) provides a different chronology of high lake levels. The presence of mud with diatomite in this core has been interpreted as representing lake highstands dating from >50 to 38 ka (Minchin), from 26 to 15 ka (Tauca), and an undated event whose age is thought to be ca. 12.5 ka (Coipasa). Detrital contamination of U-series ages and unknown ^{14}C-reservoir corrections have hindered the interpretation of many of these records.

Glaciofluvial fan deltas in Salar de Uyuni and dust and anion concentrations from the Nevado Sajama ice cap (lat 18°S) provide additional evidence for the age of lake highstands in the Salar de Coipasa–Salar de Uyuni. Concentrations of dust, sulfates, and chlorides in ice from Nevado Sajama are thought to originate from the Salar de Coipasa–Salar de

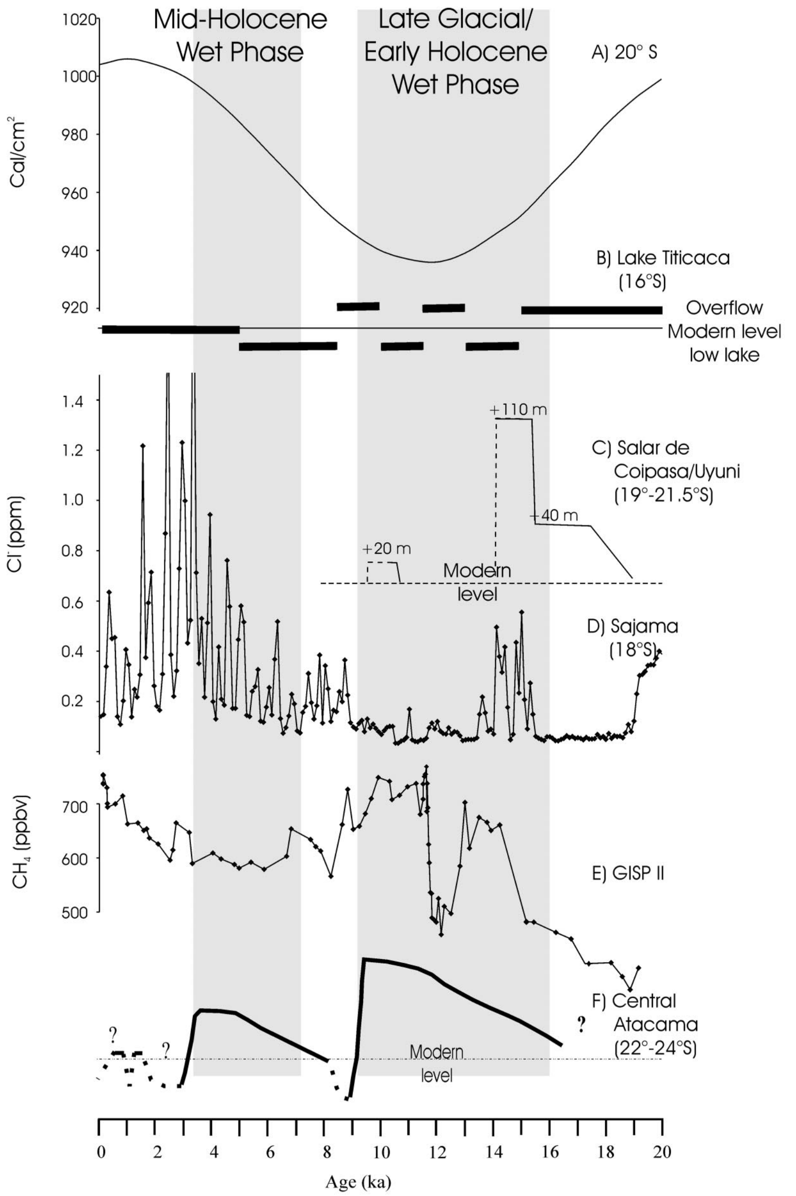

Figure 15. South American summer insolation and paleoclimatic records from the central Andes (A–D) and the global methane record (E): (A) Berger (1992), (B) Baker et al. (2001a), (C) Sylvestre et al. (1999), (D) Thompson et al. (1998), (E) Brook et al. (1996), (F) this study.

Uyuni during periods of lake desiccation (Thompson et al., 1998, 2000). The main problem with this record, however, is poor age control. AMS ^{14}C ages on organic matter within the ice provide age control at 24 ka and between 5.6 and 0 ka; however, the age of the remainder of the core is only loosely determined. Low concentrations of dust, chlorides, and sulfates suggest perennial water in the Salar de Coipasa–Salar de Uyuni prior to 22 ka (Minchin), from 21 to 15.5 ka(?), and between 14 and 9.0 ka (Tauca) (Fig. 15). After 9.0 ka, a sharp increase in chlorides, sulfates, and dust suggests lake desiccation. Glaciofluvial fan deltas south of the Salar de Coipasa are contiguous with glacial moraines and show that the last major glacial advance coincided with Glacial Lake Tauca (Clayton and Clapperton, 1997). A ^{14}C age on peat underlying glacial diamict provides a maximum age of 16.0 ka for this glacial advance.

The Amazon and the Tropics

Paleoclimatic evidence from the Amazon Basin comes primarily from sediment cores from small lakes or marshes, e.g., Lake Pata (Colinvaux et al., 1996), Carajas (Absy et al., 1991), and Salitre (Ledru, 1993), and from the Amazon Fan (Haberle and Maslin, 1999; Maslin et al., 1999) and the Ceara Rise (Harris and Mix, 1999). Pollen analyses from small lakes have been used to suggest aridity during the LGM and increased precipitation during the early Holocene; however, these conclusions remain controversial (see Colinvaux and De Oliveira, 2000). The reinterpretation of pollen diagrams from small lakes and marshes in the Amazon (Colinvaux and De Oliveira, 2000) and from the Amazon Fan (Haberle and Maslin, 1999) suggest only cooling, with minor vegetation changes between glacial and interglacial periods and do not indicate widespread aridity and a reduction in the area of tropical rain forests during the LGM. Lower lake levels and decreased sediment-deposition rates during the LGM at both Lake Pata (Colinvaux et al., 1996) and at Salitre (Ledru, 1993), however, point to lower lake levels during this time. Evidence from the Ceara Rise also indicates decreased discharge from the Amazon during glacial cycles and increased discharge during interglacial periods (Harris and Mix, 1999).

Atmospheric methane concentrations trapped in polar ice cores (Chappellaz et al., 1993; Brook et al., 1996; Steig et al., 1998) are thought to largely derive from decaying organic matter in wetlands; 40%–70% of these wetlands are located in tropical areas (Fung et al., 1991). This relationship has led researchers to use concentrations of CH_4 trapped in polar ice cores as a proxy for the extent of wetlands at tropical latitudes (Chappellaz et al., 1993; Severinghaus and Brook, 1999), although high-latitude CH_4 sources may also contribute significantly to atmospheric methane (Nisbet, 1992). The record of atmospheric CH_4 concentration from the Greenland ice cores over the past 20 k.y. identifies low methane concentrations during the LGM, a drastic rise during the late glacial, and high concentrations during the late glacial and early Holocene, except during the Younger Dryas. Methane concentrations then dropped markedly beginning at ca. 8.2 ka, remained low during the middle Holocene, and then rose during the late Holocene (Fig. 15) (Chappellaz et al. 1993; Blunier et al., 1995; Brook et al., 1996). Increased CH_4 concentrations from the late glacial through early Holocene agree well with records of increased precipitation and discharge from the central Atacama and Amazon and partially agree with the Tauca and Coipasa lake phases from the Salar de Uyuni/Coipasa.

SUMMARY AND CONCLUSION

Paleo–wetland deposits in the central Atacama Desert of northern Chile record a 16 k.y. history of regional changes in groundwater discharge. The general concordance of results from several contrasting hydrologic systems and the agreement between these records and most other paleoclimatic proxy records in the central Atacama indicate that these deposits are recording regional changes in groundwater recharge tied to long-term changes in precipitation.

The limited extent of alpine glaciers in the central Atacama during this time period precludes a significant influence of glacial meltwater on hydrologic budgets, which are thought to influence lake-level heights in more glaciated regions of the Altiplano in Bolivia and Peru. Paleo–wetland deposits from the central Atacama provide a firm chronology for the late glacial to early Holocene (>15.4–9.0 ka) wet phase in the central Atacama and also indicate a wet middle Holocene (8–3 ka), a period that was previously thought to be hyperarid. Both wet periods were terminated by pronounced dry periods, from 9 to 8 and from 3 to 0 ka, when water tables dropped and streambeds were incised. A complete lack of paleo–wetland deposits dating to the LGM suggests that water tables were low during this period, although this lack also may be the result of subsequent erosion of wetland deposits. The discordance between LGM records from large saline lakes such as the Salar de Atacama and Salar de Uyuni and records from small lakes, rodents middens, and wetland deposits in the region must reflect either temperature effects on large lake budgets or gaps in the other records. These discrepancies need to be resolved to gain a better understanding of the South American tropical climate system during the LGM.

We argue that precipitation changes in the central Atacama are directly linked to large-scale atmospheric features related to convection over the Amazon Basin, the southerly transport of moisture from the Amazon, and the transport of moisture onto and over the Altiplano. The late glacial to early Holocene wet phase in the central Atacama supports the argument for increased tropical precipitation at this time as evidenced by increased Amazon discharge (Harris and Mix, 1999) and increased atmospheric methane concentrations in polar ice cores (Chappellaz et al., 1993; Brook et al., 1996; Steig et al., 1998). Evidence of a wet late glacial to early Holocene in the central Atacama is in agreement with results from the Amazon and suggests that there was no major paleoclimatic boundary between the Amazon and Altiplano, nor between the Altiplano and the central Atacama, during the LGM and Holocene.

How the SASM is influenced by tropical SSTs, the Walker Circulation, and other large-scale features of the tropical circulation system is still poorly understood. There are many forcing mechanisms that may enhance the SASM. We agree with Sylvestre et al. (1999) and Kull and Grosjean (1998) that local summer insolation does not appear to be driving SASM intensity. Intensification of the SASM may be the result of a combination of factors, including (1) increased global temperatures driving convection over the Amazon, (2) stronger SST gradients enhancing the easterlies and therefore tropical convection (Cane et al., 2000), and (3) nonlinear responses to tropical insolation (Cane et al., 2000). Discrepancies between paleorecords from key regions influenced by the SASM need to be resolved to gain a better understanding of the interactions between the SASM and other main features of the tropical circulation system.

ACKNOWLEDGMENTS

This research was funded by National Science Foundation grant EAR-9904838 and National Geographic Society grant NGR-617898 (to Quade and Betancourt) and by a NASA space grant (to Rech). We thank Claudio Latorre, Zach Naiman, Jeff Pigati, and Christa Placzek for their field assistance. We are grateful to Latauro Núñez and everyone at the Museo Arqueologico de San Pedro de Atacama for their support. Careful reviews by Jeffrey S. Hanor and Lensyl Urbano greatly improved this manuscript.

REFERENCES CITED

Abbott, M.B., Binford, M.W., Brenner, M., and Kelts, K.R., 1997, A 3500 ^{14}C yr high-resolution record of water-level changes in Lake Titicaca, Bolivia/Peru: Quaternary Research, v. 47, p. 169–180.

Absy, M.L., Cleef, A., Fornier, M., Servant, M., Siffedine, A., Da Silva, M.F., Soubies, F., Sugio, K., Turcq, B., and van der Hammen, T., 1991, Mise en évidence de quatre phases d'ouverture de la forêt dense dans le sud-est de l'Amazonie au cours des 60,000 dernières années. Premiere comparison avec d'autres régiones tropicales: Comtes Rendus Academie Des Sciences Paris, v. 313, p. 673–678.

Aceituno, P., 1988, On the functioning of the Southern Oscillation in the South American sector. Part I: Surface climate: Monthly Weather Review, v. 116, p. 505–524.

Aceituno, P., and Montecinos, A., 1993, Circulation anomalies associated with dry and wet periods in the South American Altiplano: Proceedings of the fourth international conference on Southern Hemisphere meteorology, Hobart, Australia: American Meteorological Society, p. 330–331.

Aravena, R., and Suzuki, O., 1990, Isotopic evolution of river water in the northern Chile region: Water Resources Research, v. 26, p. 2887–2895.

Baker, P.A., Seltzer, G.O., Fritz, S.C., Dunbar, R.B., Grove, M.J., Tapia, P.M., Cross, S.L., Rowe, H.D., and Broda, J.P., 2001a, The history of South American tropical precipitation for the past 25,000 years: Science, v. 291, p. 640–643.

Baker, P.A., Rigsby, C.A., Seltzer, G.O., Fritz, S.C., Lowenstein, T.K., Bacher, N.P., and Veliz, C., 2001b, Tropical climate changes at millennial and orbital timescales on the Bolivian Altiplano: Nature, v. 409, p. 698–701.

Berger, A., 1992, Orbital variations and insolation database: Boulder, Colorado, USA, IGBP PAGES/World Data Center-A for Paleoclimatology Data Contribution Series 92–007, NOAA/NGDC Paleoclimatology Program.

Betancourt, J.L., Latorre, C., Rech, J.A., Quade, J., and Rylander, K.A., 2000, A 22,000-year record of monsoonal precipitation from northern Chile's Atacama Desert: Science, v. 289, p. 1542–1546.

Blunier, T., Chappellaz, J., Schwander, J., Stauffer, B., and Raynaud, D., 1995, Variations in atmospheric methane concentration during the Holocene Epoch: Nature, v. 374, p. 46–49.

Bobst, A.L., Lowenstein, T.K., Jordan, T.E., Godfrey, L.V., Hein, M.C., Ku, T.-L., and Luo, S., 2001, A 106 ka paleoclimatic record from the Salar de Atacama, northern Chile: Palaeogeography, Palaeoclimatology, Palaeoecology, v. 173, p. 21–42.

Brook, E.J., Sowers, T., and Orchardo, J., 1996, Rapid variations in atmospheric methane concentration during the past 110,000 years: Science, v. 273, p. 1087–1091.

Bush, A.B.G., and Philander, S.G.H., 1998, The role of the ocean-atmosphere interactions in tropical cooling during the Last Glacial Maximum: Science, v. 279, p. 1341–1344.

Cane, M.A., and Clement, A.C., 1999, A role for the tropical Pacific coupled ocean-atmosphere system on Milankovitch and millennial timescales. Part II: Global impacts, *in* Clark, P.U., Webb, R.S., and Keigwin, L.D., eds., Mechanisms of global climate change at millennial time scales: American Geophysical Union Geophysical Monograph 112, p. 373–383.

Cane, M.A., Clement, A., Gagan, M.K., Ayliffe, L.K., Tudhope, S., 2000, ENSO through the Holocene, depicted in corals and model simulation: Pages newsletter, v. 8 (1), p. 3–7.

Chappellaz, J., Blunier, T., Raynaud, D., Barnola, J.M., Schwander, J., and Stauffer, B., 1993, Synchronous changes in atmospheric CH_4 and Greenland climate between 40 and 8 kyr BP: Nature, v. 366, p. 443–445.

Clayton, J.D., and Clapperton, C.M., 1997, Broad synchrony of a late glacial glacier advance and the highstand of paleolake Tauca in the Bolivian Altiplano: Journal of Quaternary Science, v. 12, p. 169–182.

Clement, A.C., and Cane, M.A., 1999, A role for the tropical Pacific coupled ocean-atmosphere system on Milankovitch and millennial timescales. Part I: A modeling study of tropical Pacific variability, *in* Clark, P.U., Webb, R.S., and Keigwin, L.D., eds., Mechanisms of global climate change at millennial time scales: American Geophysical Union Geophysical Monograph 112, p. 373–383.

Colinvaux, P.A., and De Oliveira, P.E., 2000, Palaeoecology and climate of the Amazon basin during the last glacial cycle: Journal of Quaternary Science, v. 15, p. 347–356.

Colinvaux, P.A., De Oliveira, P.E., Moreno, J.E., Miller, M.C., and Bush, M.B., 1996, A long pollen record from lowland Amazonia: Forest and cooling and in glacial times: Science, v. 247, p. 85–88.

Cross, S.L., Baker, P.A., Seltzer, G.O., Fritz, S.C., and Dunbar, R.B., 2000, A new estimate of the Holocene lowstand level of Lake Titicaca, central Andes, and implications for tropical hydrology: The Holocene, v. 10, p. 21–32.

Dirección General de Aguas, no date, Precipitation data for region II: Santiago Chile, Ministerio de Obras Públicas, no pages.

Fritz, P.C., Silva, C., Suzuki, O., and Saltai, E., 1978, Isotope hydrology in northern Chile, *in* Proceedings of the symposium on isotope hydrology: Vienna, Austria, International Atomic Energy Agency, p. 525–543.

Fung, I., John, J., Lerner, J., Matthews, E., Praither, M., Steele, L.P., and Fraser, P.J., 1991, Three-dimensional

model synthesis of the global methane cycle: Journal of Geophysical Research, v. 96, p. 13033–13065.
Geyh, M.A., Grosjean, M., Núñez, L.A., and Schotterer, U., 1999, Radiocarbon reservoir effect and the timing of the Late-Glacial/early Holocene humid phase in the Atacama Desert (northern Chile): Quaternary Research, v. 52, p. 143–153.
Grosjean, M., 1994, Paleohydrology of Laguna Lejía (north Chilean Altiplano) and climatic implications for late-glacial times: Palaeogeography, Palaeoclimatology, Palaeoecology, v. 109, p. 89–100.
Grosjean, M., and Núñez, L., 1994, Late glacial, early and middle Holocene environments, human occupation, and resource use in the Atacama (northern Chile): Geoarchaeology: An International Journal, v. 9, p. 271–286.
Grosjean, M., Messerli, B., Ammann, C., Geyh, M., Graf, K., Jenny, B., Kammer, K., Núñez, L., Schrier, H., Schotterer, U., Schwalb, A., Valero-Garcés, B., and Vuille, M., 1995, Holocene environmental changes in the Atacama Altiplano and paleoclimatic implications: Bulletin de l'Institute Française des Études Andines, v. 24, p. 585–594.
Grosjean, M., Núñez, L., Cartajena, I., and Messerli, B., 1997, Mid-Holocene climate and culture change in the Atacama Desert, northern Chile: Quaternary Research, v. 48, p. 239–246.
Grosjean, M., van Leeuwen, J.F.N., van der Knapp, W.O., Geyh, M.A., Ammann, B., Tanner, W., Messerli, B., Núñez, L.A., Valero-Garcés, B.L., and Veit, H., 2000, A 22,000 ^{14}C year BP sediment and pollen record of climate change from Laguna Miscanti (23°S), northern Chile: Global and Planetary Change, v. 28, p. 35–51.
Haberle, S.G., and Maslin, M.A., 1999, Late Quaternary vegetation and climate change in the Amazon basin based on a 50,000 year pollen record from the Amazon fan, ODP Site 932: Quaternary Research, v. 51, p. 27–38.
Hardy, D.R., Vuille, M., Braun, C., Keimig, F., and Bradley, R.S., 1998, Annual and daily meteorological cycles at high altitude on a tropical mountain: Bulletin of the American Meteorological Society, v. 79, p. 1899–1913.
Harris, S.E., and Mix, A.C., 1999, Pleistocene precipitation balance in the Amazon basin recorded in deep sea sediments: Quaternary Research, v. 51, p. 14–26.
Hostetler, S.W., and Mix, A.C., 1999, Reassessment of ice-age cooling of the tropical ocean and atmosphere: Nature, v. 399, p. 673–676.
Kerr, R.A., 2001, The tropics return to the climate system: Science, v. 292, p. 660–661.
Kull, C., and Grosjean, M., 1998, Albedo changes, Milankovitch forcing, and late Quaternary climate change in the central Andes: Climate Dynamics, v. 14, p. 871–881.
Latorre, C.L., Betancourt, J.L., and Rylander, K.A., and Quade, J., 2002, Vegetation invasions into absolute desert: A 45,000-yr rodent midden record from the Calama–Salar de Atacama basins, northern Chile (22°–24°S): Geological Society of America Bulletin, v. 114, p. 349–366.
Ledru, M.-P., 1993, Late Quaternary environmental and climatic changes in central Brazil: Quaternary Research, v. 39, p. 90–98.
Lenters, J.D., and Cook, K.H., 1997, On the origin of the Bolivian high and related circulation features of the South American climate: Journal of Atmospheric Sciences, v. 54, p. 656–677.
Lenters, J.D., and Cook, K.H., 1999, Summertime precipitation over South America: Role of the large-scale circulation: Monthly Weather Review, v. 127, p. 409–431.
Lynch, T.F., and Stevenson, C.M., 1992, Obsidian hydration dating and temperature controls in the Punta Negra region of northern Chile: Quaternary Research, v. 37, p. 117–124.
Martin, L., Bertaux, J., Correge, T., Ledru, M.-P., Mourguiart, P., Sifeddine, A., Soubies, F., Wirrmann, D., Suguio, K., and Turcq, B., 1997, Astronomical forcing of contrasting rainfall changes in tropical South America between 12,400 and 8800 cal yr B.P.: Quaternary Research, v. 47, p. 117–122.
Maslin, M.A., Durham, E., Burns, S.J., Platzman, E., Grootes, P., Greig, S.E.J., Nadeau, M-J., Schleicher, M., Pfaulmann, U., Lomax, B., and Rimington, N., 1999, Palaeoreconstruction of the Amazon river fresh water and sediment discharge using sediments recovered at Site 942 on the Amazon fan: Journal of Quaternary Science, v. 15, p. 419–434.
Miller, A., 1976, The climate of Chile, *in* Schwerdtfeger, W., ed., Climates of central and South America: World Survey of Climatology, v. 12, p. 113–130.
Nisbet, E.G., 1992, Sources of atmospheric CH_4 in early postglacial time: Journal of Geophysical Research, v. 97, p. 12859–12867.
Nogués-Paegle, J., and Mo, K.C., 1997, Alternating wet and dry conditions over South America during summer: Monthly Weather Review, v. 125, p. 279–291.
Pinot, S., Ramstein, G., Harrison, S.P., Prentice, I.C., Guiot, J., Stute, M., and Joussaume, S., 1999, Tropical paleoclimates at the Last Glacial Maximum: Comparison of paleoclimate modeling intercomparison project (PMIP) simulations and paleodata: Climate Dynamics, v. 15, p. 857–874.
Quade, J., Forester, R.M., Pratt, W.L., and Carter, C., 1998, Black mats, spring-fed streams, and late-glacial-age recharge in the southern Great Basin: Quaternary Research, v. 49, p. 129–148.
Rech, J.A., and Pigati, J.S., 2000, Evidence for a wet mid-Holocene from Quebrada Puripica, central Atacama Desert, Chile: Geological Society of America Abstracts with Programs, v. 32, no. 7, p. A-274.
Ronchail, J., 1995, Variabilidad interanual de las precipitaciones en Bolivia: Bulletin de l'Institute Française des Études Andines, v. 24, p. 369–378.
Rondeau, B., 1990, Géochimie isotopique et géochronologie des stromatolites lacustres quaternaires de l'Altiplano bolivien [Ph.D. thesis]: Montreal, Université du Québec, 100 p.
Seltzer, G., Rodbell, D., and Burns, S., 2000, Isotopic evidence of late Quaternary climate change in tropical South America: Geology, v. 28, p. 35–38.
Servant, M., and Fontes, J.C., 1978, Les lacs quaternaires des hauts plateaux des Andes boliviennes. Premières interprétations paléoclimatiques: Cahiers ORSTOM, Sér. Géologie, v. 10, p. 9–23.
Servant, M., Fournier, M., Argollo, M., Servant-Vildary, S., Sylvestre, F., Wirrmann, D., and Ybert, J.P., 1995, La dernière transition glaciaire/interglaciaire des Andes tropicales du sud (Bolivie) d'après l'étude des variations des niveaux lacustres et des fluctuations glaciaires: Comptes Rendus Académie des Sciences Paris, v. 320, p. 729–736.
Severinghaus, J.P., and Brook, E.J., 1999, Abrupt climate change at the end of the last glacial period inferred from trapped air in polar ice: Science, v. 286, p. 930–934.
Silva Dias, P.L., Schubert, W.H., and DeMaria, M., 1983, Large-scale response of the tropical atmosphere to transient convection: Journal of Atmospheric Sciences, v. 40, p. 2689–2707.
Steig, E.J., Brook, E.J., White, W.C., Sucher, C.M., Bender, M.L., Lehman, S.J., Morse, D.L., Waddington, E.D., and Clow, G.D., 1998, Synchronous climate changes in Antarctica and the North Atlantic: Science, v. 282, p. 92–95.
Stuiver, M., and Reimer, P.J., 1993, Extended ^{14}C database and revised CALIB radiocarbon calibration program: Radiocarbon, v. 35, p. 215–230.
Stuiver, M., Reimer, P.J., Bard, E., Beck, J.W., Burr, G.S., Hughen, K.A., Kromer, B., McCormick, G., van der Plicht, J., and Spurk, M., 1998, INTCAL98 radiocarbon age calibration: Radiocarbon, v. 40, p. 1041–1083.
Sylvestre, F., Servant, M., Servant-Vildray, S., Causse, C., Fournier, M., and Ybert, J.-P., 1999, Lake-level chronology on the southern Bolivian Altiplano (18°–23°S) during late-glacial time and the early Holocene: Quaternary Research, v. 51, p. 54–66.
Thompson, L.G., Davis, M.E., Mosley-Thompson, E., Sowers, T.A., Henderson, K.A., Zagorodnov, V.S., Lin, P.-N., Mikhalenko, V.N., Campen, R.K., Bolzan, J.F., and Cole-Dai, J., 1998, A 25,000-year tropical climate history from the Bolivian ice cores: Science, v. 282, p. 1858–1864.
Thompson, L.G., Mosley-Thompson, E., and Henderson, K.A., 2000, Ice-core paleoclimate records in tropical South America since Last Glacial Maximum: Journal of Quaternary Science, v. 15, p. 377–94.
Valero-Garcés, B., Grosjean, M., Schwalb, A., Geyh, M., Messerli, B., and Kelts, K., 1996, Limnology of Laguna Miscanti: Evidence for mid to late Holocene moisture changes in the Atacama Altiplano (northern Chile): Journal of Paleolimnology, v. 16, p. 1–21.
Vuille, M., 1999, Atmospheric circulation over the Bolivian Altiplano during dry and wet periods and extreme phases of the southern oscillation: International Journal of Climatology, v. 19, p. 1579–1600.
Vuille, M., and Ammann, C., 1997, Regional snowfall patterns in the high, arid Andes: Climatic Change, v. 36, p. 413–423.
Vuille, M., and Baumgartner, M.F., 1998, Monitoring the regional and temporal variability of winter snowfall in the arid Andes using digital NOAA/AVHRR data: Geocarto International, v. 13, p. 59–67.
Vuille, M., Hardy, D.R., Braun, C., Keimig, F., and Bradley, R.S., 1998, Atmospheric circulation anomalies associated with the 1996/1997 summer precipitation events on Sajama ice cap, Bolivia: Journal of Geophysical Research, v. 103, p. 11191–11204.
Vuille, M., Bradley, R.S., and Keimig, F., 2000, Interannual climate variability in the central Andes and its relation to tropical Pacific and Atlantic forcing: Journal of Geophysical Research, v. 105, p. 12447–12466.
Wirrmann, D., and de Oliveira Almeida, L.F., 1987, Low Holocene level (7700–3650 yr ago) of Lake Titicaca (Bolivia): Palaeogeography, Palaeoclimatology, Palaeoecology, v. 59, p. 315–23.
Wirrmann, D., and Mourguiart, P., 1995, late Quaternary spatio-temporal limnological variations in the Altiplano of Bolivia: Quaternary Research, v. 43, p. 344–354.
Ybert, J.P., 1992, Ancient lake environments as deduced from pollen analysis, *in* Dejoux, C., and Iltis, A., eds., Lake Titicaca: A synthesis of limnological knowledge: Dordrecht, Netherlands, Kluwer Academic, p. 49–62.
Zhou, J., and Lau, K.-M., 1998, Does a monsoon climate exist over South America: Journal of Climate, v. 11, p. 1020–40.

Manuscript Received by the Society November 10, 2000
Revised Manuscript Received June 13, 2001
Manuscript Accepted August 24, 2001

Printed in the USA